Alma Mater Studiorum - Università di Bologna

SCUOLA DI SCIENZE

Dipartimento di Chimica Industriale "Toso Montanari"

Corso di Laurea Magistrale in

Chimica Industriale

Classe LM-71 - Scienze e Tecnologie della Chimica Industriale

Synthesis, Characterization and Conformational Studies of Bis-phenothiazine-aryl-boranes

Tesi di laurea sperimentale

CANDIDATO

Ilaria Silenzi

RELATORE

Prof. Dr. Andrea Mazzanti

CORRELATORE

Dr. Michele Mancinelli

Daniel Pecorari

Anno Accademico 2018-2019

ABSTRACT

This thesis project presents a work based on the study of a particular class of amino-boranes, called bis-phenothiazine-aryl-boranes. The peculiarity of these compounds is the N-B-N chemical moiety and their complex conformational behaviour, due to the combination of steric hindrance and conjugation of the B-N bond. Our work is focused on two main products with different symmetry: bis-phenothiazine-2-methylnaphthyl-borane (**2b**) and bis-phenothiazine-anthracenyl-borane (**2c**).

We firstly focused our attention on an effective way of synthesis, by optimizing both reaction conditions and purification. The products and co-products of interest were then characterized with NMR, mass spectroscopy and X-Ray diffraction on single crystals. The products were eventually analysed through conformational studies, by experimental techniques, such as Dynamic NMR and EXSY, and by a theorical approach with DFT calculations.

SOMMARIO

Questo progetto di tesi si è basato sullo studio di una specifica tipologia di ammino-borani, in particolare i bis-fenotiazina-aril-borani. La peculiarità di questi composti è data dal sistema N-B-N e dal loro particolare comportamento conformazionale, dovuto alla combinazione di aspetti di natura coniugativa B-N e sterica. Il nostro lavoro si è focalizzato su due prodotti a differente grado di simmetria: il bis-fenothiazina-2-metil-naftile-borano (**2b**) e il bis-fenotiazina-antracenil-borano (**2c**).

Inizialmente, sono state proposte e studiate varie vie di sintesi e di purificazione. Successivamente, sia i prodotti desiderati, che alcuni co-prodotti considerati rilevanti, sono stati caratterizzati attraverso l'uso di spettroscopia NMR e di massa, mentre, per quanto riguarda i singoli cristalli, essi sono stati analizzati mediante diffrazione a raggi X. Infine, sono stati svolti degli studi legati alle differenti conformazioni dei prodotti e alle loro rispettive energie sia attraverso analisi sperimentali, come la dinamica NMR e l'EXSY, sia con studi teorici computazionali mediante calcoli DFT.

INDEX

1 Introduction

1.1 Aminoboranes

In the last few years, aminoboranes has gained consistency as a new field of research in chemistry. The peculiar feature of these compounds is the presence of a boron-nitrogen bond which is highly interesting, since it is isosteric and isoelectronic to a carbon-carbon double bond.

This kind of molecules belong to the so called "smart"[1] materials since their physical and chemical properties allow them to go through reversible transformations as a result of one or more external stimuli (e.g. light,[2] heat,[3] pressure,[4] electric field,[5] pH,[6,7] viscosity[8] or presence of other molecules[9]), or physical changes (e.g. phase transition,[10] isomerism[11] or intermolecular interactions[12]).

These functional materials turn out to be a compelling branch of research for practical applications. In fact, they can have a role as fluorescent sensors, organic-light emitting diodes (OLEDs), organic lasers exc.[13] Classical organic luminophores such as pyrene, anthracene and triphenylamine show bright luminescence in solution, but they exhibit a poor emission quantum yield when they are in solid state or in highly concentrated solutions by the notorious effect of aggregation-caused quenching (ACQ). On the contrary, aminoboranes exhibit aggregation-induced emission (AIE) and they can work as mega-Stokes-shift dyes; structural rigidification and bulky groups further increasing these features. The source of these features is the electron deficiency of boron: its empty p_z orbital allows to establish a π-conjugation with a smaller HOMO-LUMO gap, thus producing new photophysical properties to the molecule. On the other side, amino-group is electron-rich, so it can act as donor to provide the formation of the double bond.

The study of these molecules is also interesting in the perspective of designing new medicines since the B-N bond is included in a broad-spectrum modulator of various membrane proteins.[14] Generally, most of the medicines turn out to be highly effective on the human body when they are optically active. Hence, it would be interesting to deepen a study on chiral aminoboranes, especially focusing on atropoisomeric ones, so that it is possible to study the rotational energy barrier of boron-carbon axis.

1.2 Chirality

Stereoisomerism is defined as a feature of molecules with the same atomic connectivity but different arrangement of atoms within space. Stereoisomerism, in turn, can be either conformational (compounds can be interconverted by the rotation about single bonds) or configurational (arrangements of atoms of a molecular entity in space that distinguishes stereoisomers). If configurational stereoisomers are non-superimposable mirror images, they are called enantiomers, vice versa they are diastereoisomers. Enantiomeric molecules are also defined as chiral. This word derives from the Greek, "χειρ (kheir)": this expression was firstly adopted by Lord Kelvin in 1904 and it means "hand", as a way to explain the concept with an everyday chiral object. The most common type of organic chemistry chirality is characterised by a carbon atom bearing four different substituents: carbon is the stereogenic centre, all substituents have the same connectivity, but they can have different disposition in the space. Another possible source of chirality is determined by the presence of a chiral axis: a rotation around this axis can convert one conformational enantiomer into its mirror image. In these cases, the stability of the two enantiomers to racemization is related to the energy barrier for rotation around the chiral axis.

One of first scientists who focused his studies on the complexity of stereochemistry was Louis Pasteur, who declared the famous sentence about the chirality of the universe: "*l'univers est dissymetrique*".[15] Chirality plays an essential role in a lot of natural mechanisms: synthesis, functioning of enzymes, effectiveness of drugs, exc. Biologically active amino acids and carbohydrates belong to a single absolute configuration. Therefore, active sites of enzymes are able to recognize and work only with a particular stereoisomer. For example, cholesterol could have 256 stereoisomers, but only one is synthetized by the biological process. Another intriguing consequence is that, even if they have the same chemical and physical properties, enantiomers can affect the human body in a completely different way. A striking event in the history was the use of racemic thalidomide as a sedative and anti-nausea drug for pregnant women, until it was discovered that if one of the enantiomer had the expected result, the other one was teratogen for the foetus.[16] Hence, the importance of researching new synthetic and analytic ways to obtain and characterize singular pure enantiomers was clear.

1.3 Atropisomerism

Atropisomers are a class of chiral compounds characterised by the frozen rotation of σ-bonds with an energy barrier larger than 21.8 kcal/mol,[17] which results in a half-life of >1000 s at +25 °C. Atropisomers often result from a hindered rotation of bonds connecting two aromatic rings giving an axial chirality (Figure **1.a**) or from a barrier in the ring flip of a medium-sized ring resulting as a planar chirality (Figure **1.b**).
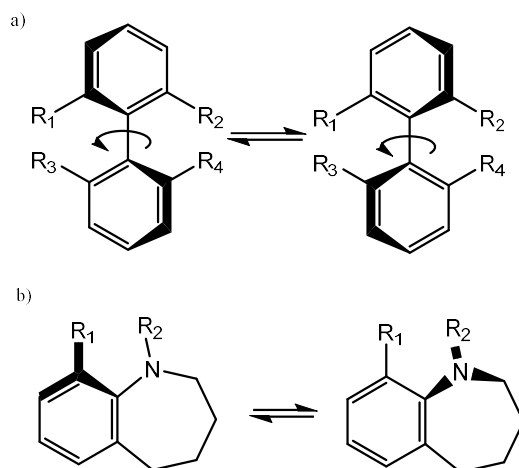
Figure 1 : Figures 1a and 1b are examples of atropisomers with axial or planar chirality

Depending on the overall structure of the molecule, atropisomers can form either enantiomers or diastereomers. Racemization occurs by a bond rotation and the activation energy of this process is a result of electron distribution, solvent, temperature and steric hindrance. The higher the barrier is, more stable are the two enantiomers.
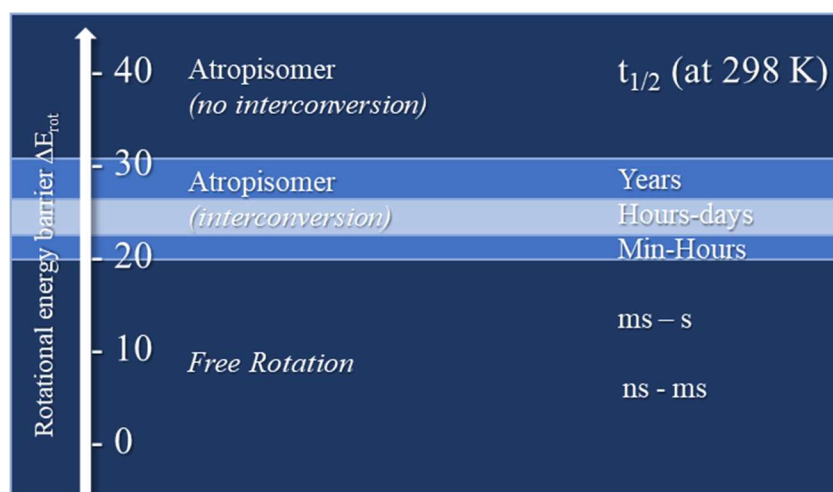
Figure 2 Energy barrier with relative half-life time at +25 °C of a single atropisomers

3

LaPlante and co-workers[18] proposed some guidelines for the drug development of atropisomers, based on the rotational energy barriers. Depending on the case, atropisomers can be divided in three classes, as reported in Figure **2**.

- *Class 1*: ΔE_{rot} < 20 kcal/mol, $t_{1/2}$ of minutes. These compounds have fast axial rotation rates, therefore they should be treated as a single compound, since the resolution and the individual bioactivity assessment would be too challenging.

- *Class 2*: ΔE_{rot} 20–30 kcal/mol range, $t_{1/2}$ of hours to days. In this area, isolation of a single compound is really challenging since it is not completely stable. Only if the energetic barriers are between 23 kcal/mol and 30 kcal/mol, these products could be resolved and stored as a single enantiomerically pure atropisomer for hours or weeks at temperature of +25 °C.

- *Class 3*: ΔE_{rot} ≥ 30 kcal/mol, $t_{1/2}$ in years. Atropisomers should be easily separated: they are kinetically stable and no axial rotation is expected to occur at +25 °C.

This classification is not completely strict, but rather there can be halfway situations, especially because rotational barriers depend on more than one factor. For example, the value of rotational barrier energy of a molecule in liquid solution is lower than in solid state. In the same way, crystalline and amorphous state can also be different, since the crystalline structure has a strictly defined packing. Moreover, all the energy barriers are calculated at room temperature, to better understand the stability of atropisomers, but it is fundamental to remember that rotation is highly influenced by the temperature, and the drugs work at the temperature of the human body. In fact, in contrast to classical chiral compounds, as the temperature increases, the molecule owns enough energy to overcome the energy barrier and to be able to freely rotate, and then the two conformations result indistinguishable.

Another remarkable feature is the nomenclature of the absolute configuration of the atropisomers. It is based on the priority of the atoms that constitute the dihedral angle of the chiral axis. Dihedral angle is described by four atoms A, B, C and D (Figure 3) and it is generated by the intersection of two planes: one made up of the points A, B and C, where A has higher priority than the other atom connected to B, and the other described by the points B, C and D, where D is chosen for the same reason of A. The nomenclature is determined by looking at the B-C axis and placing atom A closer to the observer, so that, depending on the position of atom D it is possible to describe an angle and determine the configuration P - plus (clockwise) or M - minus (counterclockwise).
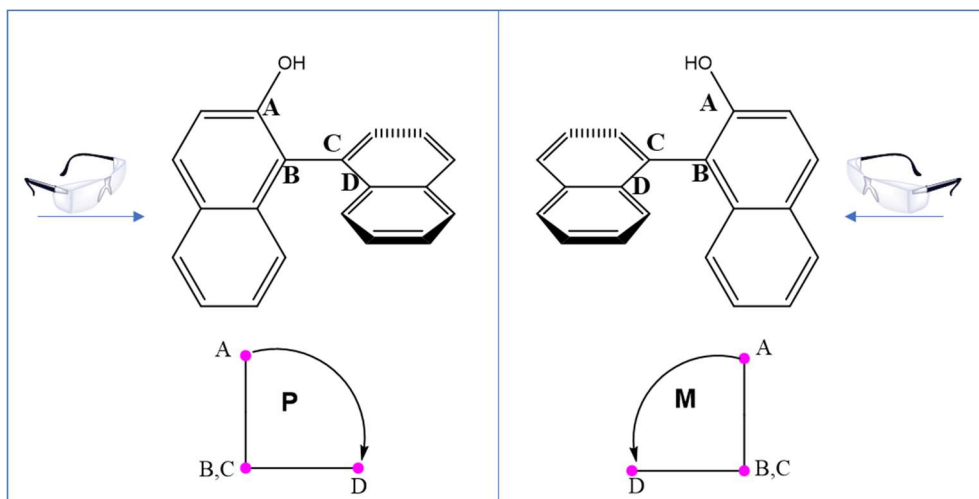
Figure 3 Representation of the dihedral angle and scheme of its nomenclature

1.4 Molecular Propellers

When a molecule is composed by a single atomic centre, such as Boron, connected to two or more aryl rings, rotation about the B-C bond axis by one of the aryl rings is substantially influenced by the other rings. Although, the torsion angle of any ring is free to rotate, the torsion of two or more internal rotors (two-ring flip) provokes a constraint among the torsion angles of all the three rings. Hence, none of the rings moves independently from the others. This synergic motion is also called correlated rotation.[19] As a result, each ring should be imagined as a blade of a propeller: each blade is twisted in the same sense, to give a helical conformation to the molecule.

Triaryl molecules (where the central atom can be a boron or the isoelectronic carbocation) are an example of molecular propellers and they are necessarily chiral and may be asymmetric if properly modified with some substituents. Then, any of these molecules must exhibit two enantiomeric forms. Diastereomeric forms are also possible, depending on the substitution pattern.
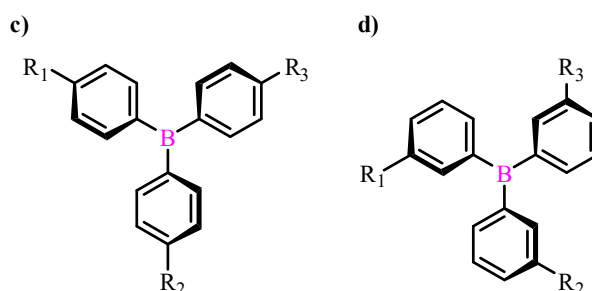
Figure 4 Examples of triarylboranes

5

For example, in Figure **4** there are two possible triarylboranes. The aryl substituents (R_1, R_2 and R_3) are different from each other and they do not contain elements of stereoisomerism, structure **4c**. It can have only two enantiomers, since the sense of the molecular propeller could be right-handed or left-handed. In case **4d** the situation is a bit more complex, in fact, if we consider the plane made up of the three carbon atoms directly connected to the central boron, it can be noticed that each substituent could situate either above or below the plane, for a total of 2^4 stereoisomeric forms, namely eight diastereomeric pairs.

A reason why molecular propellers is a compelling branch of study is due to the high similarity, even if in a microscopic way, to the fascinating and revolutionary molecular machines, for which the 2016 Nobel Prize was awarded. In fact, if nowadays molecular machines are employed on solid surfaces such as molecular vehicles, the ability of molecular scale blades of propellers to rotate around their axis could be more and more developed.[20] In this perspective, further research of molecular machines demands accurate and robust design of molecular propellers with precise control over their rotation direction.

In nature, molecular propellers play a fundamental role in a variety of biological applications, such as the swimming of bacteria and intracellular transport. The advantage of producing synthetic molecular propellers is the possibility for them to be employed in harsher environments than natural ones.

In case of molecular propellers, the description of the stereochemistry is a bit more complex than classical biphenyls, since the incident planes are less evident. Hence, it is necessary to consider the planes leading on the "blade" of the propeller, keeping one of them closer to the observer (Figure 5, red plane). Depending on the direction of the other plane (blue) and following the smallest angle given by the incidence of two planes it is possible to define if the stereochemistry is *M* or *P*. Herein we have an example with a similar molecule to the one presented in the article of Zhang and co-workers.[20]
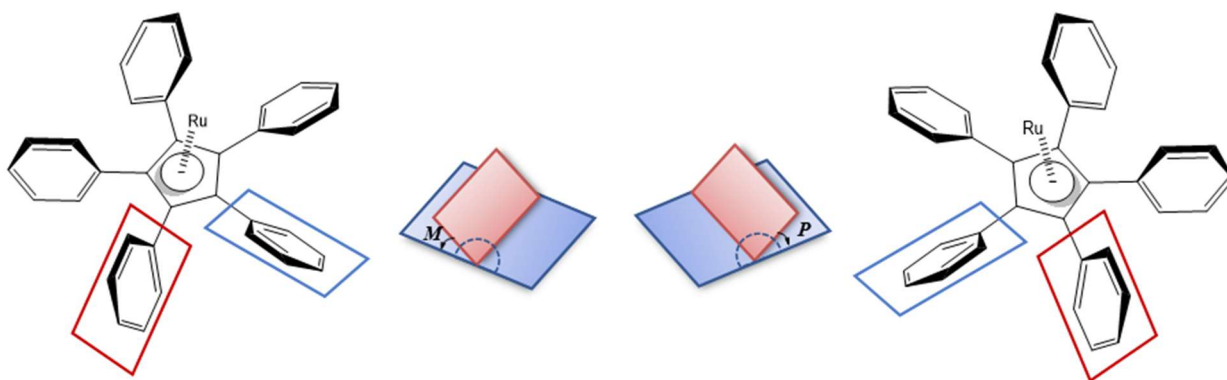
Figure 5 Stereochemistry of propellers

1.5 Diarylboryl-Phenothiazine based molecules

One of the class of molecules which received a particular attention in the latest years is amino-aryl-boranes. A first study was done by Thiligar and co-workers,[21] who developed the synthesis for a diarylboryl-phenothiazine. This product belongs to the smart materials previously cited in the first part of the introduction, since they are both amino-boranes and they also include another heteroatom (S). In fact, doped systems tend to have superior optical and electronic properties compared to the simple hydrocarbon systems.

The proposed synthesis is reported in Scheme 1.
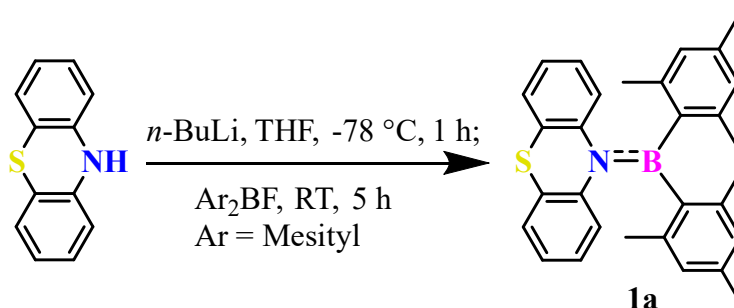
Scheme 1 Synthesis of compound 1a

Compound **1a** was synthetized by the deprotonation and lithiation of phenothiazine with 1 equivalent of *n*-BuLi at -78 °C, followed by a nucleophilic attack to dimesitylboronfluoride. This product results to be stable under ambient conditions and thermally stable up to +250 °C. Several properties are exhibited by this compound, such as triboluminescence, mechanofluorochromism, temperature sensing, aggregation induced emission (AIE) and bright solid-state emission. The first three properties refer to the ability of this material of being influenced by physical external stimuli. More specifically, triboluminescence and mechanofluorochromism are related to mechanical interactions. For example, triboluminescence is a particular phenomenon, where light is emitted as a result of frictional

interaction between the materials, such as rubbing, scratching, crushing or ripping. In this case it was observed, while trying to divide two crystals of the molecule. Mechanofluorochromism, instead, is based on the switching of the fluorescence spectrum in response to external forces (shearing, grinding, smearing, stretching, etc.).

Aggregation induced emission and solid-state emission rely indeed on the solid structure of the molecule itself. In particular, AIE is the property of showing stronger photoluminescence (PL) in the solid state than in dilute solution.

2 Aim of the Thesis

The purpose of this experimental thesis is the preparation and characterization of new aminoboranes with a N-B-N system, trying to find an effective synthesis and concentrating our studies on the conformational analysis and the rotational barrier energy of their interconversion. In particular, we have focused our attention on bis-phenothiazine-boranes: the characteristic non-planar butterfly-like shape of phenothiazine turns out to be an ideal donor and inhibits fluorescence quenching by π-π interaction both in solution and in solid form. As third substituent, we have chosen aryl rings with different steric hindrance, two C_2-symmetric (mesitylene and anthracene) and one asymmetric (2-methylnaphthalene). For the sake of clarity, all the products and intermediates which concern a certain aryl ring are signed with their corresponding letter: **a** for mesitylene, **b** for 2-methylnaphthalene, and **c** for anthracene.
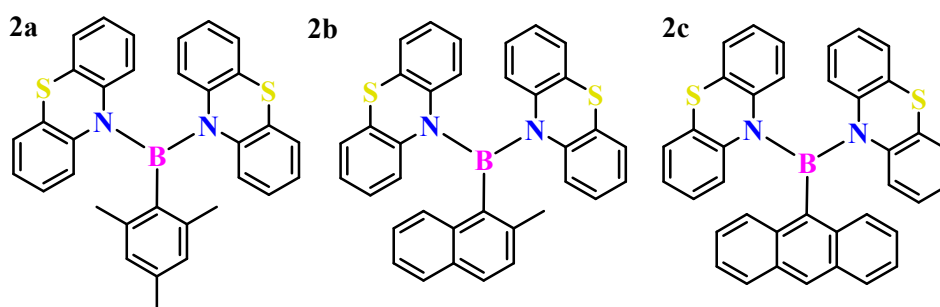
*Figure 6 Compounds **2a**, **2b** and **2c**, (from the left: bis-phenothiazine-mesityl-borane, bis-phenothiazine-2-methylnaphthyl-borane and bis-phenothiazine-anthracenyl-borane)*

Moreover, other co-products are produced (bis-aryl-boranes in particular) in the reactions and we employed them in our studies to make further considerations. For example, compounds **1b** and **1c** reported in Figure 7 (Compound **1a** is known, see above).
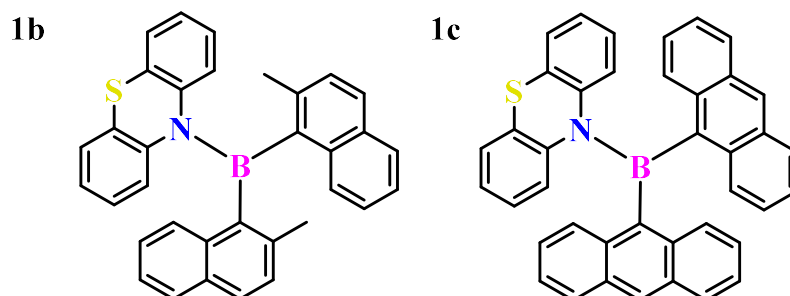
*Figure 7 Compounds **1b** and **1c** (On the left: bis-2-methyl-naphtyl-phenothiazine-borane; on the right: bis-anthracenyl-phenothiazine-borane)*

9

For any of this product, we accomplished the following analysis:

♦ Research of a good synthetic way, trying to reduce as much as possible the number of by-products, optimizing the general conditions (i.e. temperature, solvent, reaction time, stoichiometry of reagents) and purification of the final products.

♦ Characterization of the products via NMR, mass spectroscopy and X-Ray on single crystals.

♦ Computational DFT calculations have been employed to predict stable conformations of molecules and free energy values related to ground states and transition states. These calculations provide also a support for the interpretation of experimental data.

♦ Dynamic NMR and EXSY are used for the kinetic studies to determine the experimental value of rotational energy barriers.

♦ Fluorescence analysis is made to study how the maximum of emission of these compounds in solution is influenced by changing the solvent.

3   Results and Discussion

3.1   *Synthesis and Characterization*

The synthetic way to obtain the desired products was firstly inspired by the reaction proposed by Thilagar et al.[21] to prepare dimesityl-boron-phenothiazine, by changing the stoichiometric ratio to promote the formation of the bis-phenothiazine-mesityl-borane (**2a**) as reported in Scheme 1. Hence, the only changes we made compared to the reaction scheme proposed in the article was the use of 2 equivalents of phenothiazine. Firstly, we looked for the synthesis of difluoro-mesityl-borane. We followed the synthesis proposed for fluoro-mesityl-borane by Ping et al.,[22] changing stoichiometric ratio to preferentially obtain difluoro-mesityl-borane, as reported in Scheme 2.
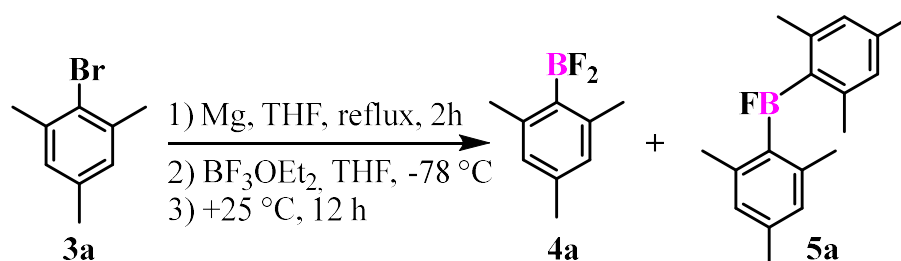
Scheme 2 Synthesis of difluoro-mesityl-borane

Even though the stoichiometric ratio was tuned to obtain difluoro-mesityl-borane (**4a**), it was anyway observed with ^{19}F-NMR analysis that both products were formed with a 3:2 ratio (**5a** : **4a**). This is probably due to the higher stability of fluoro-dimesityl-borane (**5a**). Because of the high reactivity, the two co-products were not separated, and, moreover, it was not possible to remove any residual BF$_3$ under vacuum, since difluoro-mesityl-borane (**4a**) can be easily sublimated and consequently it would be lost.

Hence, the reaction mixture was reacted with an excess of phenothiazine, in order to obtain both **1a** and **2a**. Even if several attempts were made, **1a** was the only obtained product, with a huge quantity of by-products mainly derived by oxygen attack on boron, and boronic acids. Table 1 shows the optimization attempts, trying to change solvent, base, temperature exc. Unfortunately, none of them yielded **2a**.

As shown in Table 1, even the yields of **1a** are really low. Since our laboratory is not provided with glovebox, it is quite difficult to maintain a perfect inert reaction environment and the probability of quenching is rather relevant.

Therefore, we looked for another synthetic way with different aryl substituents (as anthracenyl and 2-metyl-naphthyl). Firstly, we followed the same reaction scheme proposed by the article, but after many attempts, we concluded that the best reaction pathway was the one shown in Scheme 3.

Table 1 Reaction trials for 1a and 2a

Reaction	Solvent	Temperature (°C)	Base	Boron Reactant	Yield **1a** (%)	Yield **2a** (%)
IS1	THF	-78 to RT	n-BuLi	$BF_3 \cdot OEt_2$	13	0
IS2	THF	RT	KHMDS	$BF_3 \cdot OEt_2$	18	0
IS3	Toluene	Reflux	KHMDS	$BF_3 \cdot OEt_2$	9	0
IS4	Toluene	Reflux	KHMDS	BCl_3	0	0
IS5	Et_2O	Reflux	KHMDS	$BF_3 \cdot OEt_2$	0	0
IS6	CPME	Reflux	KHMDS	$BF_3 \cdot OEt_2$	2	0
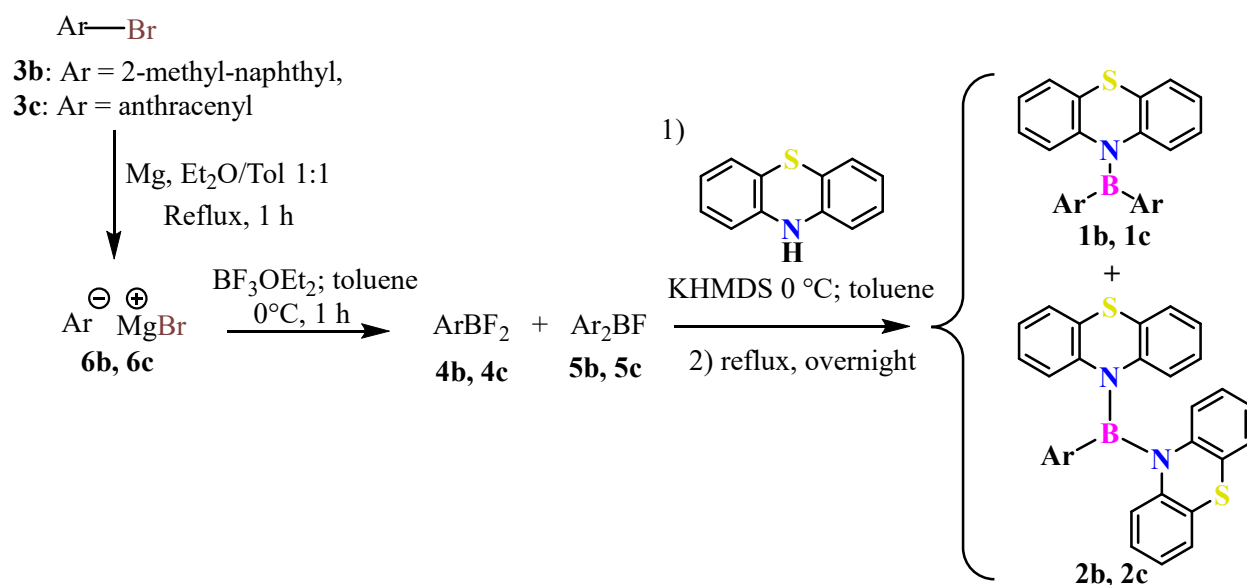
Scheme 3 Reaction scheme adopted for 1b, 1c, 2b, 2c

Compared to the reaction reported in the literature, instead of using n-BuLi, we opted for a more sterically hindered strong base as KHMDS: its non-nucleophilic nature turns out to be more effective in deprotonations, especially for secondary amines like phenothiazine. Moreover, since we noticed how THF could provide the formation of further by-products, we

attempted the employment of other solvents, toluene resulting the best one, with even a better yield (both for 2-methyl-naphthyl and for anthracenyl products) than THF.

It is fundamental to underline that all the reactions must be conducted under inert atmosphere, in our case nitrogen was employed. In fact, this kind of reactions are usually done using glovebox, since the intermediates produced (**4**, **5** and **6**) are quite unstable in the air. The synthetic way starts from the formation of Grignard reagents (**6**), using aryl-bromide (**3**) and magnesium. Since these aryl rings have a significant steric hindrance, magnesium must be highly activated and used in excess: to do that magnesium is left stirring for one night in diethyl ether and toluene 1:1 at room temperature. As already said, steric hindrance makes it difficult to react immediately: to overcome this problem, a catalytic amount of iodine is added, and the temperature increased until reflux. If the reaction starts it will be visible a sharp colour change from a deep orange/red to a yellow solution. It must be noticed that this Grignard preparation with diethyl ether and toluene 1:1 is useless in the case of mesitylene and this is probably due to the steric hindrance imposed by the presence of the two *ortho* methyls, that makes it harder to react.

Once the Grignard is obtained, the reaction mixture results to be quite turbid and with a yellow brown colour (both for 2-methylnaphthalene and anthracene). Diethyl ether must be removed under vacuum or it will provide the formation of ethers by-products. After evaporation, the residue was dissolved in the same amount of toluene. At this point, $BF_3 \cdot OEt_2$ is added to the mixture at 0 °C and left it reacting for about 30 minutes under reflux. As soon as $BF_3 \cdot OEt_2$ is added, the reaction mixture becomes suddenly limpid, as a signal that the reaction is fast and that both Ar_2BF and $ArBF_2$ are highly soluble in toluene. At this step there is also a relevant formation of triaryl borane. To overcome this problem and to support the formation of $ArBF_2$, it was tried to reverse the reactants by adding the Grignard into a solution of $BF_3 \cdot OEt_2$ in toluene, so that $BF_3 \cdot OEt_2$ will be always in excess, but this procedure was hampered by the insolubility of the Grignard in this solvent and there was not a relevant change in terms of yield and by-products. Hence, the only improvement we could do was the addition of $BF_3 \cdot OEt_2$ at 0 °C in order to make the reaction as slow as possible. Even slower temperatures were tried but with no substantial difference.

When the reaction is complete, the solution is collected with a syringe to separate it from the non-reacted magnesium and it is dried under vacuum to remove any residual BF_3. Once that it is completely dried, phenothiazine is added and soon after dry toluene is replaced as solvent. Everything is stirred until the solid becomes completely soluble in toluene. The last step is the

addition of the base KHMDS at 0 °C and then the mixture is brought under reflux by night, so that phenothiazine is deprotonated, and the nucleophilic substitution occurs.

The same reaction was tried with other reactants, but the products were not formed at all. For example, instead of using $BF_3 \cdot OEt_2$ we attempted to employ BCl_3 without success. As already said, n-BuLi was used at -78 °C as reported in the article but one of the majority by-products was the butyl-phenothiazine and the desired products were not formed at all.

All the results are summarised in Table 2.

*Table 2 Reaction trials for **1b, 2b, 1c, 2c***

Reaction	Solvent	Temperature (°C)	Base	Boron Reactant	Yield **1b** %	Yield **2b** %	Yield **1c** %	Yield **2c** %
IS7	THF	-78 to RT	n-BuLi	$BF_3 \cdot OEt_2$	//	//	0	0
IS8	THF	-78 to RT	KHMDS	$BF_3 \cdot OEt_2$	< 1	< 1	2	1
IS9	Toluene	Reflux	KHMDS	$BF_3 \cdot OEt_2$	24	13	8	5
IS10	Toluene	Reflux	KHMDS	BCl_3	//	//	0	0
IS11	CPME	Reflux	KHMDS	$BF_3 \cdot OEt_2$	//	//	0	0

// = reaction not done

Even if various possibilities were tried, these products were not easily synthesizable, and the only positive combination was IS9.

The workup of reaction mixture was done by filtrating the solution on a plug of Celite® and it was washed with CH_2Cl_2 to be sure of dissolving all the organic phase. Both in case of 2-methylnaphtil and anthracenyl reaction, the filtered solution takes on a brownish colour. The purification of the final products was firstly done with a silica chromatography column using as solvent a solution of n-Hexane/CH_2Cl_2 with an 8:2 ratio. Since the yields were often low, it was also necessary a further purification with a preparative HPLC using a direct phase column with n-Hexane/CH_2Cl_2 90:10 as eluent. All the products and by-products were analysed with NMR, in deuterated acetonitrile or CD_2Cl_2.

The pure products were then crystallized from a solution of ACN/CH₂Cl₂ 5:1 at room temperature, so that it was possible to confirm their structure with X-Ray diffraction (as shown in Figure **8**).
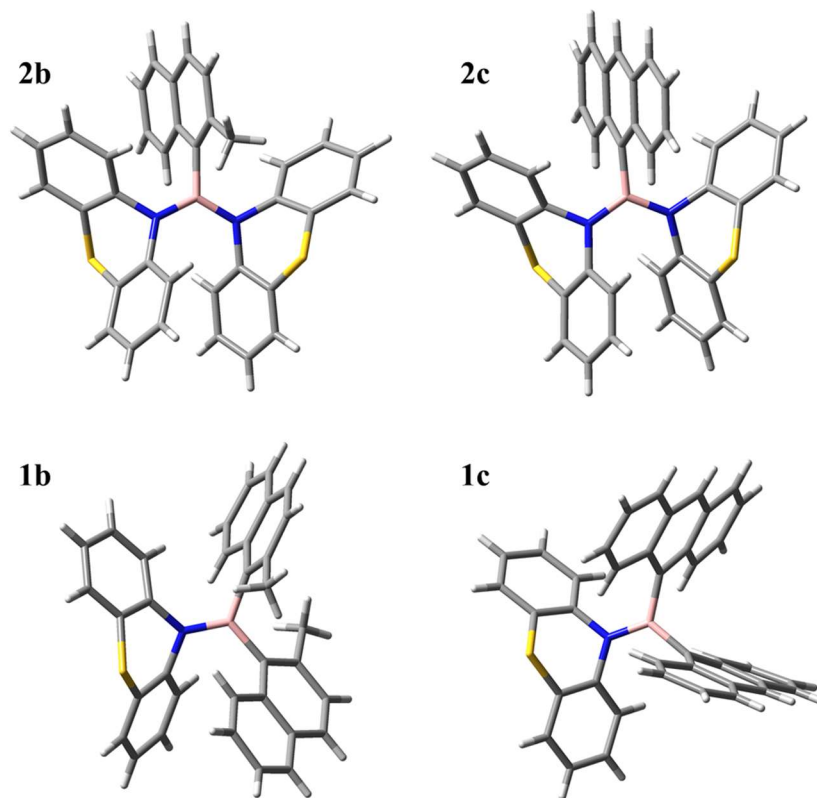
Figure 8 X-Rays Structures

All the reaction mixtures presented a relevant quantity of non-reacted phenothiazine, not only because it was added in excess, but also because a remarkable number of parasitic reactions took place. Most of them leaded to boronic acids, and they were highly recognizable due to their characteristic pink colour. Two interesting by-products, which were formed with both aryl rings are the ethoxy-boranes **7b** and **7c**.
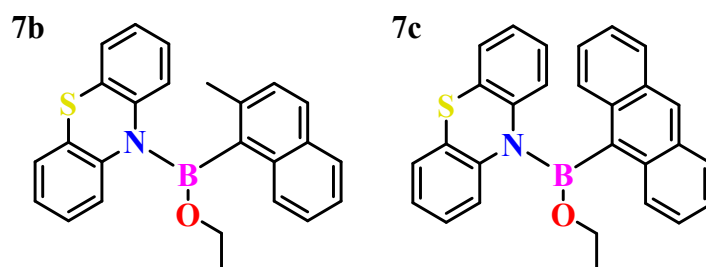
*Figure 9 By-products **7b** and **7c***

The presence of these by-products was probably caused by the ethers included in $BF_3 \cdot OEt_2$, since all the diethyl-ether used to promote the formation of Grignard was removed under vacuum before the addition of $BF_3 \cdot OEt_2$ and it would be unlikely to think that it was not completely removed considering its high volatility. Moreover, it is easy to imagine how a nucleophilic attack by OEt^- group on Boron would be favoured, compared to a more sterically hindered anion such as phenothiazine.

Other by-products were particularly challenging to identify since the NMR spectrum resulted quite complex. With the mass-spectroscopy analysis it was found out that most of them had a molecular weight greater than 800 g/mol, therefore we associated these high values to a more complex B-O-B system, probably caused by condensation of two Ar_2BOH molecules.

3.2 Conformational Studies and DFT Calculation

The X-Ray analysis allows to define unequivocally the molecular structures, but it is important to consider that the crystallographic packing could be completely different from the effective conformation of the molecule in solution, where more than one conformation could be populated. For this reason, it is possible to resort to density functional theory (DFT) to predict the stable conformations of molecules and their transition states in a pretty accurate way.

In particular we used one of the most well-known functionals, which is the B3LYP,[23] using the 6-311G(d,p) basis set, in order to obtain good accuracy. For any of our molecules, we identified all the possible ground states and transition states[24].

Our strategy to identify all the possible transition states was the positioning of the three rings in a parallel or perpendicular disposition to the plane defined by boron and the three atoms directly bonded, with all the possible combinations: one-ring flip, two-ring flip and three-ring flip (see above for the definition of ring-flip). For example, in case of one-ring flip, one ring is perpendicular to boron plane, while the other two are parallel. The zero-ring flip, which entails all the three rings on the boron plane, is not possible for any of the four molecules because it would be too sterically hindered.

Moreover, another characteristic motion of these molecules is given by the inversion of the butterfly-like structure of phenothiazine, which we will call Phen-flip. The minimum value calculated among the transition states corresponds to the free energy rotational barrier that can be compared with the experimental one. To better study the conformations of our molecules it

is important to account for further considerations. In fact, there is a substantial difference with the classical propellers (see Figure **4**), since the phenothiazine ring is not planar like a polyaromatic carbon ring. For this reason, we found out a strategy to define uniquely the configurations. We considered the concavity direction of phenothiazine like it was a blade of an anemometer, where the third aromatic ring is the pivot for rotation: as the "wind blows" the rotation direction will due to the different concavity of the Phenothiazine rings, and it can be clockwise (*r*) or counterclockwise (*s*), Figure **10**. Hence, the molecules **2b** and **2c**, in the *anti*-configurations (see below), can both have a couple of enantiomers that can be distinguishable with this method. As an assumption, the B-C bond must be placed behind. An example, considering the structure of **2b** is shown in Figure **10**.
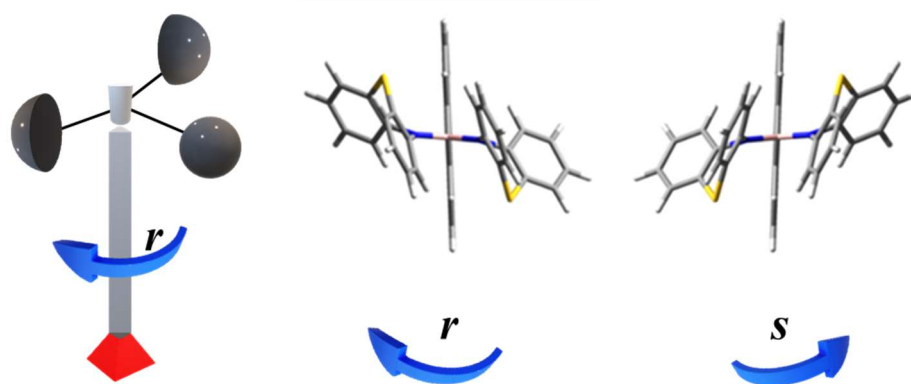
Figure 10 Stereochemistry of "anemometers" molecules

These conformations would be distinguishable if the energy barrier of the molecule is bigger than 20 kcal/mol. A technique to determine experimentally the energy barrier is dynamic NMR, which studies the variation of the NMR spectrum on changing the temperature. In, particular, the peaks that should be analysed are those that show a different multiplicity depending on the rotational rate they have. After the experimental spectra are acquired, a line shape simulation program is used to determine the rate constants for the dynamic process, and hence, through the Eyring equation, the $\Delta G^{\neq}$ value is obtained. The program used for this simulation is DNMR-6 QCPE n°633 (Dynamic Nuclear magnetic Resonance - Quantum Chemistry Program Exchange).

Dynamic NMR is not always the best technique to evaluate this energy, especially when it would cause an overlapping of multiple signals, making the spectrum too complex to be analysed. Another available technique for the kinetic study is EXSY (Exchange Spectroscopy) analysis: it requires the irradiation of a single peak with the same pulse sequences of NOESY, but with a smaller mixing time, nearly in the scale of milliseconds. In

this evolution time, the nearest protons do not develop NOE effect, while the proton irradiated can exchange its position in the space and interchange with another and exhibit itself in the spectrum. It is thus possible to see the amount of signal exchanged in function of the mixing time by simple integration. The interpolation of these values by a first-order reversible kinetic treatment will provide the rate constant of the phenomenon and hence the activation energy $\Delta G^{\neq}$. In the following paragraphs all the conformational studies made with DFT calculation are described, and then it is shown the experimental analysis on the different molecules by DNMR for **1c**, both DNMR and EXSY for **1b** and by EXSY for **2b** and **2c**.

To better understand the schematization used to describe the transition states, here it is presented a little legend.
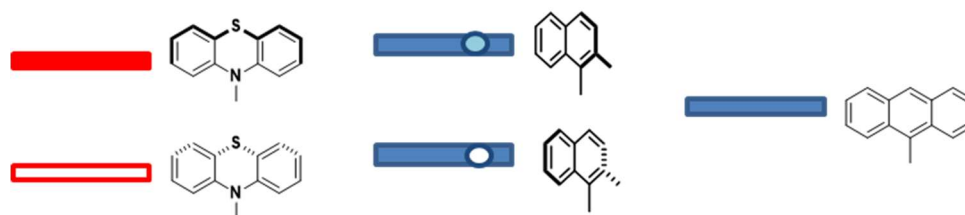
Figure 11 Legend for the representation of molecules

3.2.1 DFT Calculations for bis-anthracenyl-phenothiazine-borane 1c

Having two anthracenyl groups instead of methyl-naphthyls, **1c** is a molecule with a more symmetric structure than **1b**, hence there are less possibilities of conformations and transition states (Table 3). It has an only ground state where the anthracenyl rings are in helical conformation, which gives a combination of steric and conjugative stability.

One-ring-flip transition states are only two since all the other possibilities would lead to enantiomeric forms which are energetically identical, or, in case of **TS3-1rf** (1rf = one ring flip), the steric hindrance is too demanding. The one-ring-flip transition states are determined by the rotation and distortion of the anthracenyl ring, with the bending of the quaternary carbon and they are both similar in energy. **TS1-1rf** is the most probable to happen.

TS1-2rf (4.20 kcal/mol) is the transition state with whom **GS1** converts its enantiomeric conformations in a very fast way, and it presents a C_S symmetry, but the energy value is very small, and not experimentally observable. **TS2-2rf** (19.97 kcal/mol**)** and **TS3-2rf** (31.68 kcal/mol) refer to the phenothiazine rotation. They have both one anthracenyl ring on the plane but in case of **TS3-2rf** the concavity of phenothiazine causes its distortion and so it is much higher in energy, hence only **TS2-2rf** would be observable.

Three-ring-flip transition state geometries were not found, since they demand both steric hindrance and the loss of boron-nitrogen conjugation.

Phen-flip-TS is the other transition state which can exchange the two enantiomeric conformations of **GS1** with a calculated energy barrier of 11.82 kcal/mol. Being this barrier much lower than **TS1-1rf** (21.63 kcal/mol), it is feasible to measure it by dynamic NMR observing the two side of anthracene that may be near or far from S.

19

Table 3 GSs and TSs for 1c
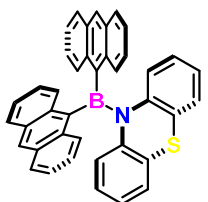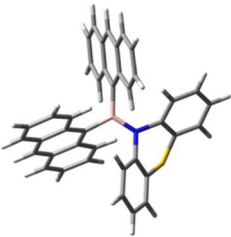
	Schematic Rapresentation	3D Structure	Total Energy (a.u.)	Rel. E. Calcd. (kcal/mol)
GS1			-2017.695895	0.00
TS1-1rf			-2017.661419	**<u>21.63</u>**
TS2-1rf			-2017.659049	23.12
TS3-1rf		Too much steric hindrance	//	//
TS1-2rf			-2017.689194	**<u>4.20</u>**
TS2-2rf			-2017.664075	**<u>19.97</u>**
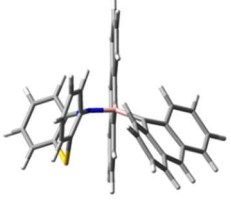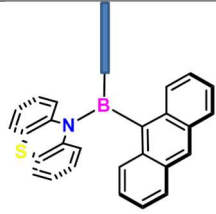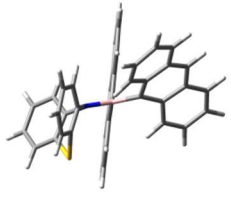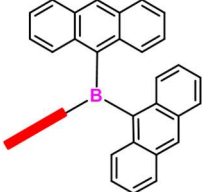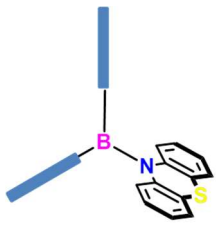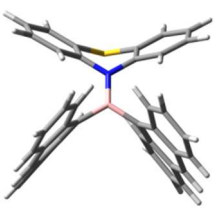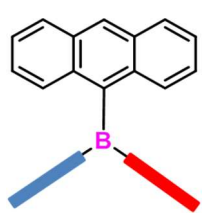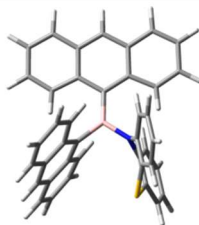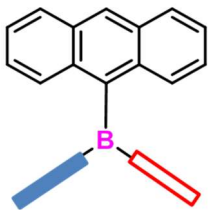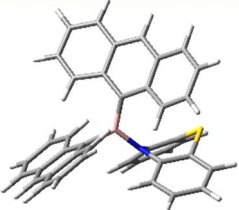
TS3-2rf			-2017.645407	31.68
TS1-3rf		Not found	//	//
TS2-3rf		Not found	//	//
TS-Phen-flip			-2017.677055	**<u>11.82</u>**
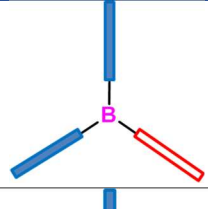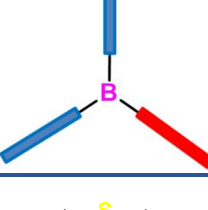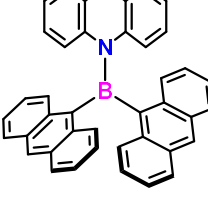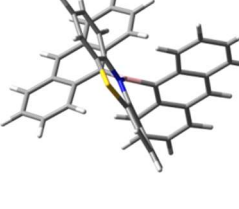
3.2.2 DFT Calculations for bis-2-methyl-naphtyl-phenothiazine-borane 1b

Compound **1b** presents three ground states, where the three substituents of boron are in an helicoidal conformation, with the phenothiazine above or below the boron plane (Table 4). This disposition of the rings is the most favourable, especially where the methyls of the naphthalene rings are in *anti*-position. A further stabilization is given by the conjugation B-N, so that the doublet of nitrogen is aligned with the empty orbital of boron. The only ground state suggested to be effectively populated is the **GS1-*anti* (99.93%)**, since, according to Boltzmann law, the **GS2-*syn*** is populated only for the 0.07% and the population of **GS3-*syn*** is even smaller.

One-ring-flip transition states are all in the order of 20-25 kcal/mol, so they all belong to class 2 (see Figure **2**). **TS1-1rf** is originated by the rotation of one naphthyl ring, therefore the two methyls become closer and the energy consequently increases (21.77 kcal/mol) compared to the **GS1-*anti*** conformation. In **TS2-1rf**, there is still the motion of the naphthyl ring, but in this case the methyl is in the opposite direction and it gets closer to the phenothiazine ring,

showing a higher energy compared to **TS1-1rf** (23.08 kcal/mol). **TS3-1rf** is also similar to **TS1-1rf**, but the naphthyl bending is opposite and, as a result, the methyls are even closer (3.36 Å vs. 3.83 Å), so the energy is higher (24.41 kcal/mol). In **TS4-1rf** the two methyls are in *anti* and the naphthyl rings have the same bending of **TS3-1rf** which is energetically disfavoured (25.01 kcal/mol). In **TS5-1rf, TS6-1rf, TS7-1rf** and **TS8-1rf** the rotation of the two naphthyl rings rotation is the same of the previous transition states, but in these cases the concavity of phenothiazine is flipped, and the energetical values keep nearly the same values (~ 23-24 kcal/mol). For what concerns **TS9-1rf,** it was not even possible to draw the 3D molecule, since it would have required the overlapping of atoms. Hence, the most probable transition state associated to the naphthyl rotation is **TS1-1rf** with a calculated value of 21.77 kcal/mol.

TS1-2rf and **TS2-2rf** correspond to the synergic movement of the two naphthyl-rings, from one enantiomer to the other, the first one is for the *syn* (5.48 kcal/mol), while the other is for the *anti* (5.38 kcal/mol). They are very fast and so, they are not experimentally observable.

The other two-ring-flip transition states refer to the phenothiazine rotation. **TS3-2rf** is the highest in energy (35.11 kcal/mol) because there is the complete loss of conjugation between boron and nitrogen, since they are perpendicular to each other. Moreover, one naphthyl ring is distorted. **TS4-2rf** (20.62 kcal/mol) presents the same loss of B-N conjugation, but the naphthyl rings are better fitted being perpendicular to each other, so they succeed in staying planar. We find a similar situation in **TS6-2rf**, but in this case, being one naphthyl turned in the other direction, it has its methyl closer to the concavity of phenothiazine, so it is a bit more energetically demanding (22.34 kcal/mol). **TS5-2rf**, instead, is more comparable to **TS3-2rf**, with a slight reduction of energy (31.64 kcal/mol) due to a better packing of the naphthyl rings. Therefore, the most likely transition state to be observed for the phenothiazine rotation is **TS4-2rf** with 20.62 kcal/mol.

Three-ring-flip transition are not easy to find, since their conformation is highly instable, and they tend to rotate one of the substituents to get to the closest transition state. For example, in case **TS2-3rf** rotates one of the naphthyl rings to obtain the same conformation of **TS5-2rf**. For **TS1-3rf** instead, it was determined a transition state, even if it doesn't keep completely all the rings perpendicular to the plane, because it would be too steric hindered to exist.

The last are the two **Phen-flip** transition states, which differentiate for the methyls in *anti* (11.84 kcal/mol) or *syn* (12.34 kcal/mol) position and they are similar in energy.

Table 4 GSs and TSs for 1b

	Schematic Rapresentation	3D structure	Total Energy (a.u.)	Rel. E. Calcd (kcal/mol)
GS1-anti			-1789.046815	0.00
GS2-syn			-1789.044094	1.71
GS3-syn			-1789.045679	0.71
TS1-1rf			-1789.012121	**21.77**
TS2-1rf			-1789.010035	23.08
TS3-1rf			-1789.007913	24.41
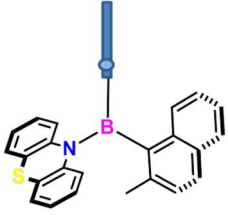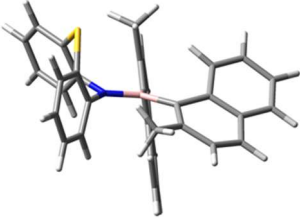
TS4-1rf			-1789.006962	25.01
TS5-1rf			-1789.008530	24.02
TS6-1rf			-1789.007943	24.39
TS7-1rf			-1789.010745	22.63
TS8-1rf			-1789.008378	24.12
TS9-1rf		Too much steric hindrance	//	//
TS1-2rf			-1789.038078	**<u>5.48</u>**
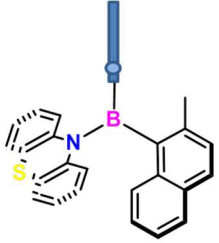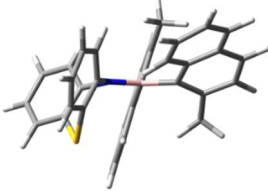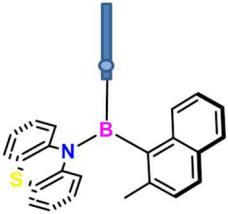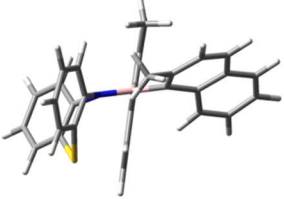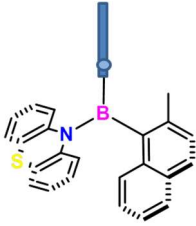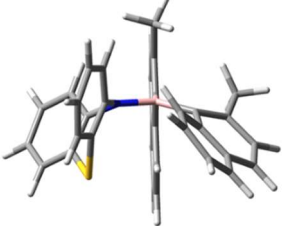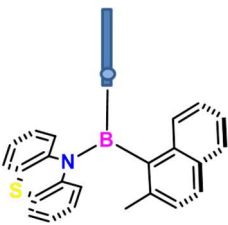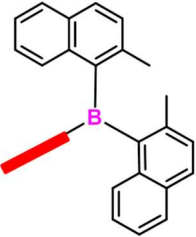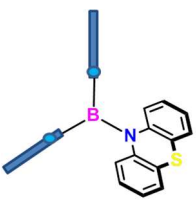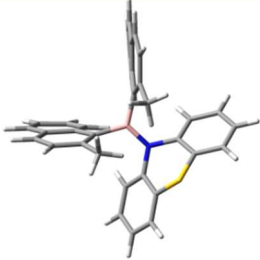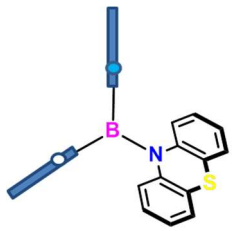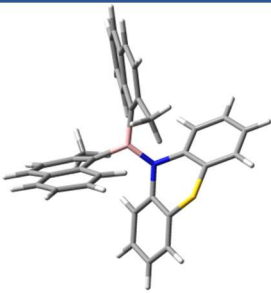
TS2-2rf			-1789.038240	**5.38**
TS3-2rf			-1788.990855	35.11
TS4-2rf			-1789.013959	**20.62**
TS5-2rf			-1788.996387	31.64
TS6-2rf			-1789.011213	22.34
TS1-3rf			-1788.993495	33.46
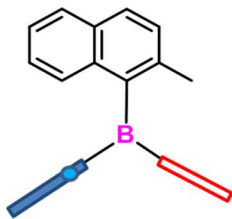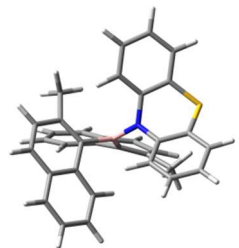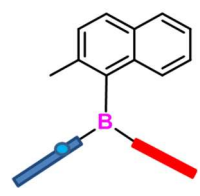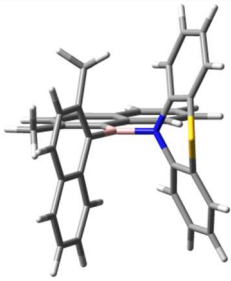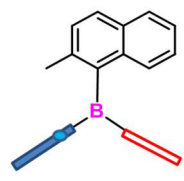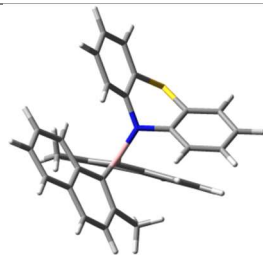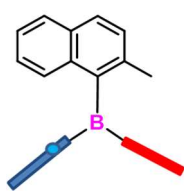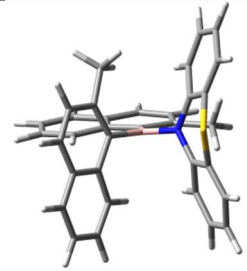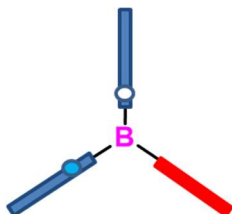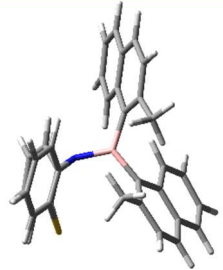
TS2-3rf		Not found	//	//
TS-Phen-flip *syn*			-1789.027941	**11.84**
TS-Phen-flip *anti*			-1789.027156	**12.34**

3.2.3 DFT Calculations for bis-phenothiazine-anthracenyl-borane 2c

Compound **2c** presents two ground states, one for the *syn*-position and one for the *anti*. From the DFT calculation, it is possible to see that the *anti*-conformation is more stable and the only populated, since the *syn* geometry is 5.24 kcal/mol. The other one-ring-flip states do not exist, because they would require the overlapping of atoms.

TS1-2rf and **TS2-2rf** shows the rotation of the phenothiazine and they differ from its concavity. The energy of the first one is slightly bigger, since there is a little distortion of the anthracenyl ring perpendicular to boron plane, hence **TS2-2rf** is the most favoured. **TS3-2rf** is the highest in energy: both phenothiazines goes perpendicular and they do not conjugate with boron. **TS4-2rf** was not found and its conformation collapsed into **TS2-2rf**.

None of the three-ring-flip was possible to find.

Phen-flip (18.91 kcal/mol) and **TS2-2rf** (16.31 kcal/mol) are the transition states that exchange the *anti* conformations, passing through the non-populated *syn* conformation. With EXSY analysis it is possible to determine only the transition state due to the phenothiazine rotation.

Table 5 GSs and TSs for 2c

	Schematic Rapresentation	3D Structure	Total Energy (a.u.)	Rel. E. Calc. (kcal/mol)
GS1-*anti*			-2393.884815	0.00
GS2-*syn*			-2393.876468	5.24
TS1-1rf		Too much steric hindrance	//	//
TS2-1rf		Too much steric hindrance	//	//
TS1-2rf			-2393.857834	16.93
TS2-2rf			-2393.858822	**<u>16.31</u>**
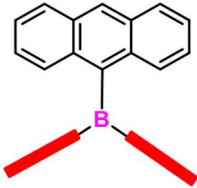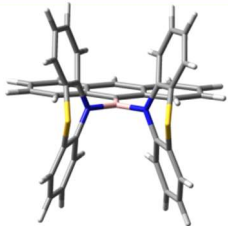
TS3-2rf			-2393.832602	32.76
TS4-2rf		Not found	//	//
TS1-3rf		Not found	//	//
TS2-3rf		Not found	//	//
TS-Phen-flip			-2393.854684	**18.91**
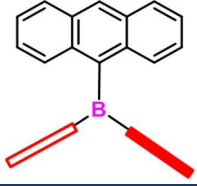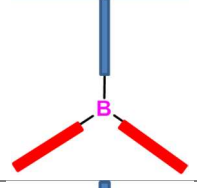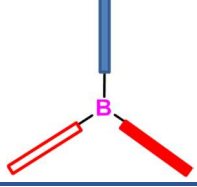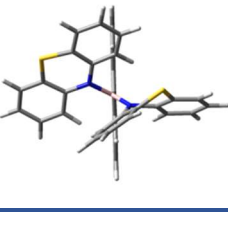
From this analysis it can be described the most favourable energy scale as shown in Figure **12**, with the rotation of the phenothiazine going through **TS2-2rf**.
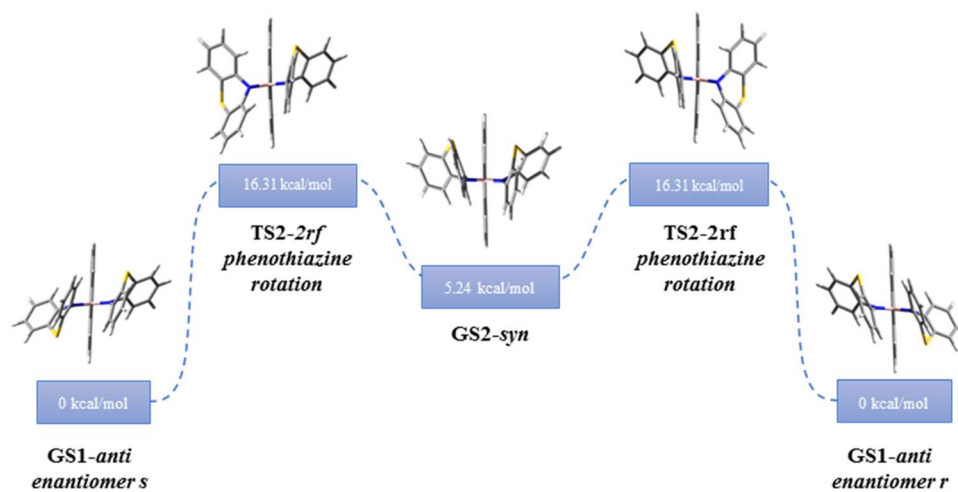
Figure 12 Energy scale for B-N rotation

3.2.4 DFT Calculations for bis-phenothiazine-2-methylnaphthyl-borane 2b

Bis-phenothiazine-2-methylnaphthyl-borane can have three ground-state conformations, since the concavity of the two phenothiazine rings can be either *anti* or *syn*. In the case of the *anti* disposition an enantiomeric pair is generated, whereas in case of *syn*, the 2-methyl-naphthyl can be placed with the methyl near the sulphur atom of phenothiazines, or far from it. Analysing the different energies, it is reasonable to think that only **GS1-*anti*** is populated. Since the 2-methyl-naphthyl ring is perpendicular to the boron plane they correspond to the one-ring-flip conformation.

Two-ring-flip process implies that at least one phenothiazine rotates and loses the boron-nitrogen conjugation. The first four transition states are quite similar, and they differ for the concavity direction of phenothiazine, but the most likely to happen is **TS3-2rf** (16.58 kcal/mol).

The other two-ring-flip processes are the most unfavoured, since both nitrogens lose conjugation with boron. In particular, **TS5-2rf** is disfavoured for conjugation, but this is balanced by a good spatial arrangement of the substituents. **TS7-2rf**, is disfavoured from any point of view, in fact it has a relative energy of 42.09 kcal/mol. **TS6-2rf** and **TS8-2rf** were not found, since they rotate the group until they reach **TS5-2rf.**

For the same reasons of excessive energetic demand, three-ring-flip transition states were not found. In case of **TS1-3rf**, makes a rotation to **GS3**, while **TS2-3rf** goes to the more stable **TS2-2rf.**

In compound **2b** the two **Phen-flip** transition states have a value of 18.62 and 20.29 kcal/mol. A consideration that should be done is that **Phen-flip** (18.62 kcal/mol) and **TS3-2rf** (16.58 kcal/mol) transition states have nearly the same energy barrier, so they will probably share the same temperature of activation (this will be successively confirmed in the EXSY analysis).

Table 6 GSs and TSs for 2b
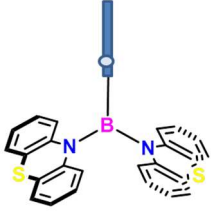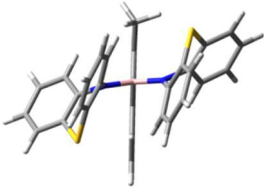
	Schematic Rapresentation	3D structure	Total Energy (a.u.)	Rel. E. Calcd (kcal/mol)
GS1 *anti*			-2279.560313	0.00
GS2 *syn*			-2279.551596	5.47
GS3 *syn*			-2279.550598	6.10
TS1-2rf			-2279.531803	17.89
TS2-2rf			-2279.530540	18.68
TS3-2rf			-2279.533893	**16.58**
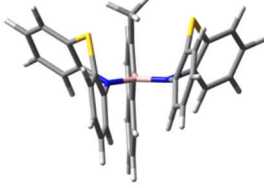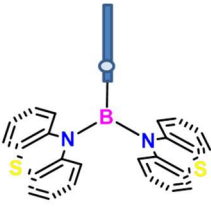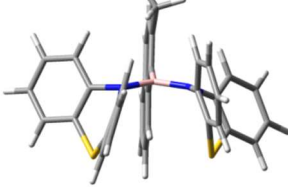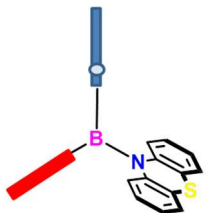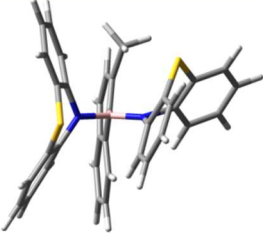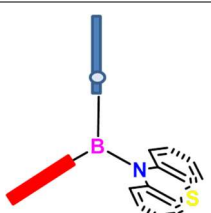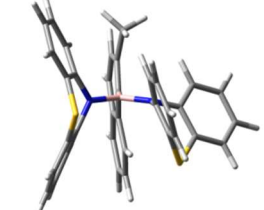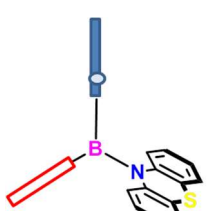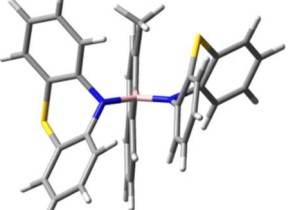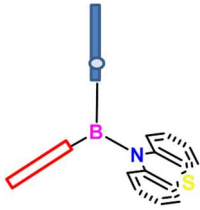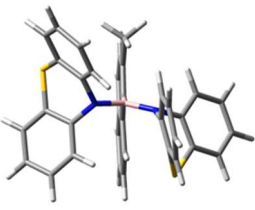
TS4-2rf			-2279.533535	16.80
TS5-2rf			-2279.506316	33.88
TS6-2rf		Not found	//	//
TS7-2rf			-2279.493234	42.09
TS8-2rf		Not found	//	//
TS1-3rf		Not found	//	//
TS2-3rf		Not found	//	//
TS1-Phen-flip			-2279.527972	20.29
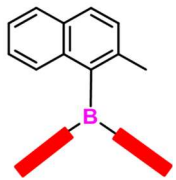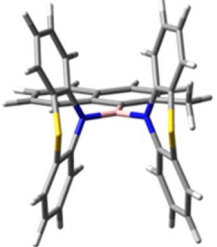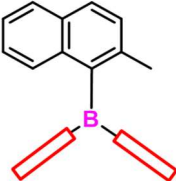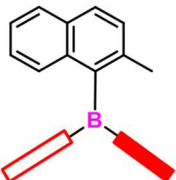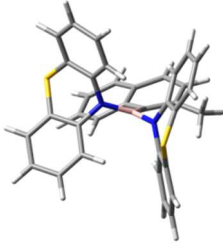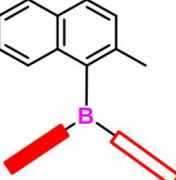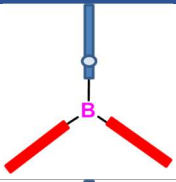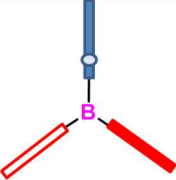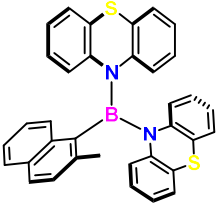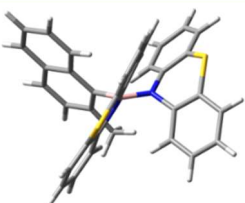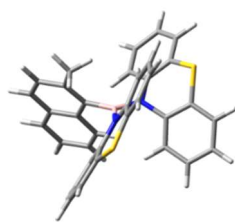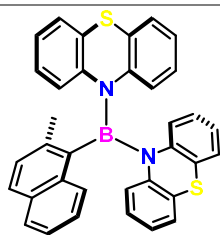
| TS2-Phen-flip | | | -2279.530643 | **18.62** |

3.2.5 *Dynamic NMR of 1c*

At +25 °C the NMR spectrum of the product **1c** (as **1b** too) shows all the anthracenyl signals as very broad signals, except for the singlet of the proton in 9-position. This means that they are in exchange between each other. As the DFT calculations confirm, the only possible movement which would cause the exchange between these protons, is the **Phen-flip**. In fact, the phenothiazine rotation around the B-N axis would require passing through too high in energy transition states, hence it would not be sterically favoured. Within this framework, the proton in 9-position is not affected by this conformational process.

On lowering the temperature, the signals broaden and reach the coalescence temperature at -2 °C. At -34 °C, the signals are completely defined. In Figure **11**, it is presented the evolution of the signal related to the protons in position 4 of the anthracene, which are characterized by a J-*ortho* and a J-*meta*. When the **Phen-flip** process is frozen, one side of the anthracene will be different from the other and, at the same time, the two anthracene will be symmetry related.

On the left of Figure **13**, it is represented the experimental spectra, the simulated ones are presented on the right. From the simulation, it is found a value of $\Delta G^{\neq}$ of 13.1±0.15 kcal/mol, which is quite similar to the one calculated for the **Phen-flip** in the DFT calculations (11.82 kcal/mol). The $\Delta G^{\neq}$ value was the average values of the $\Delta G^{\neq}$ values derived from the rate constants obtained from the line shape simulations at each temperature.

32
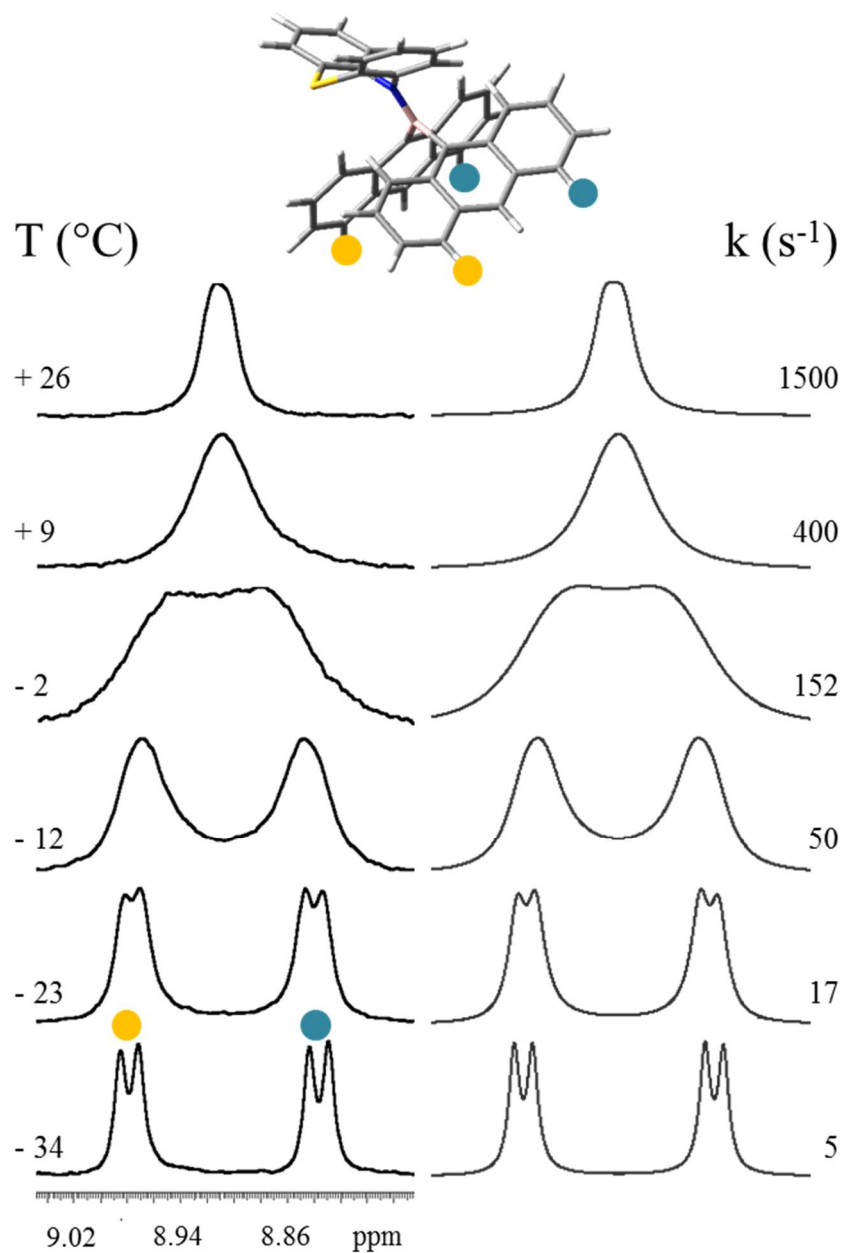
*Figure 13 DNMR of **1c**. Left: temperature dependence of the 4 anthracenyl ^1H signal in CD_2Cl_2 at 600 MHz. Right: line shape simulation obtained with the rate constants reported.*

3.2.6 1D-EXSY of 2c

Products **2c** required an EXSY analysis, because its dynamic spectrum would have presented multiple broad signals overlapping one to each other. Therefore, we decided to irradiate one of the doublets of phenothiazine with ten different mixing times. With the increasing of the mixing time, the molecule has more time to rotate and so, the signal of the other corresponding proton raises. This kind of analysis can give unequivocally the energy referred to the rotation of the phenothiazine, since the **Phen-flip** would not show any visible effect on the irradiated proton. On the other hand, in the B-N phenothiazine rotation there is an exchange between the protons of the two sides of the ammine. To better understand this process, in Figure **14** there is the schematization of the different movements.
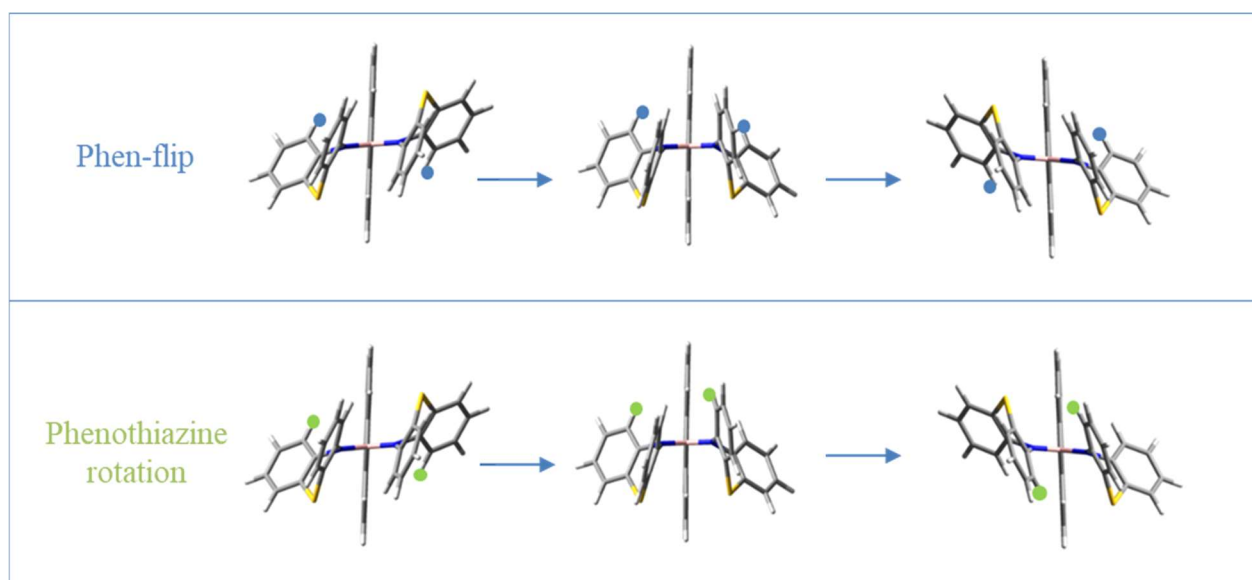
Figure 14 Difference between Phen-flip and Phenothiazine Rotation

Hence, the proton with the coloured point is irradiated with ten different mixing times and at three different temperatures (+25 °C, +27.5 °C and +30 °C). It is important to evaluate the results at more than one temperature to get a more accurate $\Delta G^{\neq}$, given by the average of the three values obtained. The EXSY experiment must be considered like a reaction with a kinetic of the first order reversible to equilibrium, where at a mixing time of 0.00 ms there is the 100% of the irradiated proton, while at an infinite time it is reached an equilibrium of 50% of irradiated proton and 50% of the exchanged proton. Figure **15** shows an example of the experiment taken at +30 °C.

				Mixing time (s)					
0.02	0.04	0.06	0.08	0.10	0.12	0.14	0.16	0.18	0.20

97.9 % 95.7 % 93.8 % 92.1 % 90.1 % 88.8 % 86.9 % 85.5 % 84.0 % 82.4 %

2.1 % 4.3 % 6.2 % 7.9 % 9.9 % 11.2 % 13.1 % 14.5 % 16.0 % 17.6 %

6.8 ppm 6.8 ppm 6.8 ppm 6.8 ppm 6.8 ppm 6.8 ppm 6.8 ppm 6.8 ppm 6.8 ppm 6.8 ppm
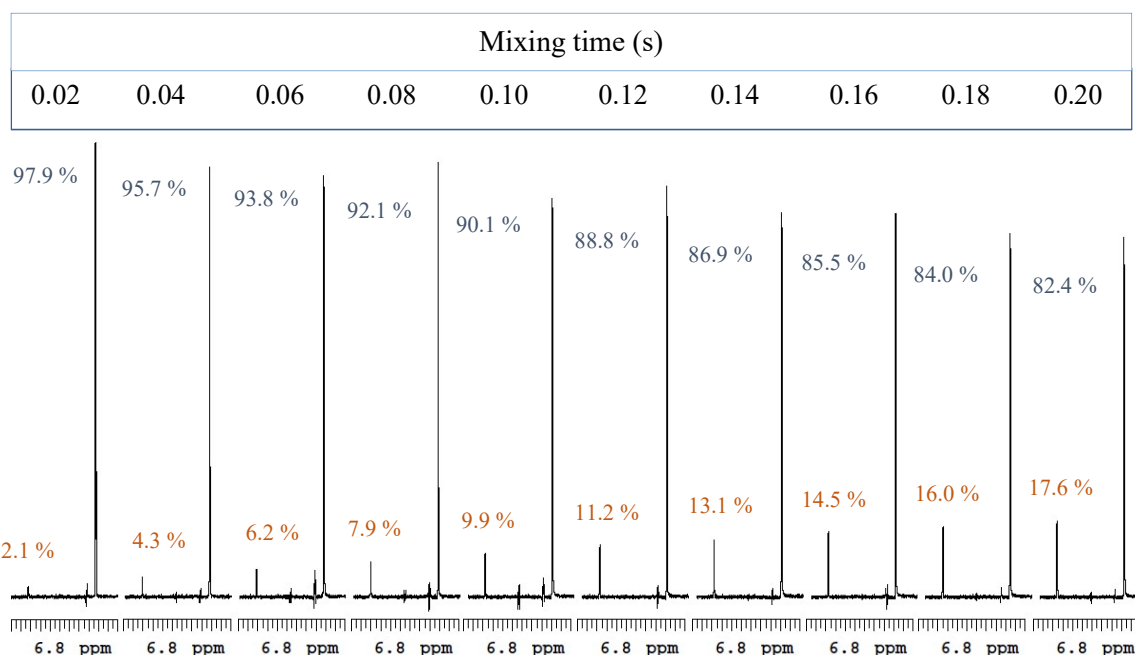
*Figure 15 EXSY of **2c** at +30 °C of the 1 phenothiazine ^{1}H signal in CD_2Cl_2 at 600 MHz*

The equation for a first-order reversible reaction at equilibrium is the following:

$$\ln\left(C_{irr} - C_{irr\,eq}\right) = -2k \cdot t_{mix} + \ln\left(C_{irr\,0} - C_{irr\,eq}\right)$$

Where C_{irr} is the percentage of the irradiated signal, $C_{irr\,eq}$ corresponds to the equilibrium (which is always 0.5 in our case), C_{irr0} is the percentage at zero time (which is always 1), t is the mixing time and k is the value of the kinetic constant. For any of the three temperature we obtained a different value of k (0.66 s^{-1}, at +25 °C, 0.86 s^{-1} at +27.5 °C and 1.07 s^{-1} at +30 °C).

y = -1,3235x - 0,6949
R² = 0,9978
25 °C

y = -1,7148x - 0,6941
R² = 0,998
27.5 °C

y = -2,1476x - 0,6945
R² = 0,9994
30 °C
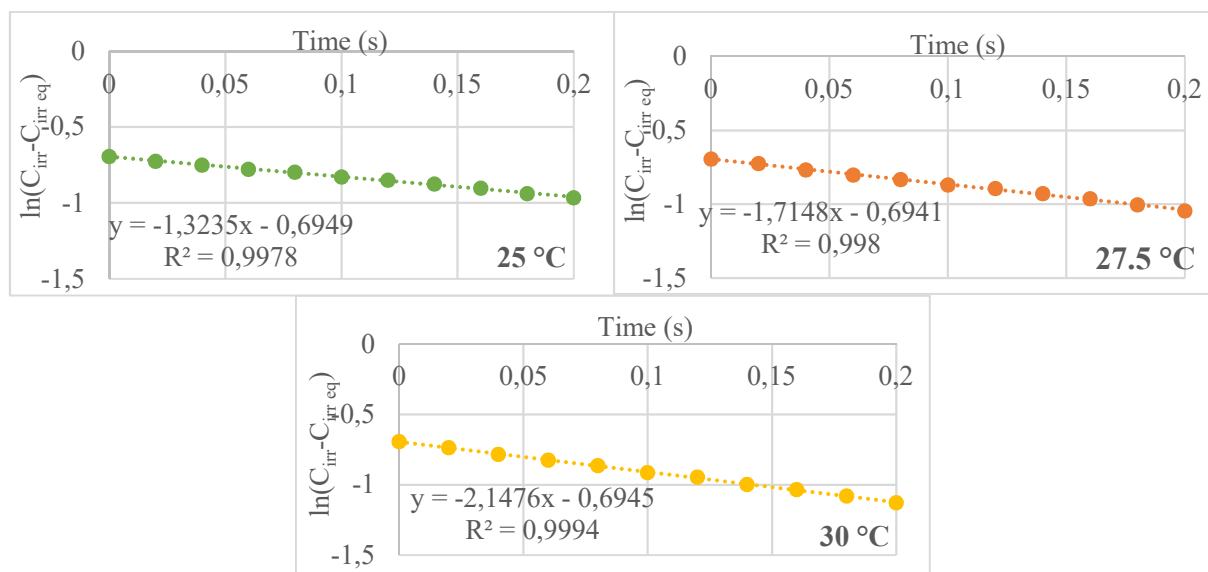
*Graphic 1 Kinetic equations from EXSY analysis for different temperatures for compound **2c***

35

The Eyring equation was used to convert the rate constant k to $\Delta G^{\neq}$, and we obtained a value of 17.7 ± 0.2 kcal/mol which is completely consistent with the results obtained with the DFT calculations for **TS2-2rf** of 16.31 kcal/mol.

Another experiment that we tried to make to further verify the possibility to obtain two separate enantiomers from this compound, was the use of the enantiopure Pirkle's alcohol (TFAE: (R)-1,1,1,trifluoro-anthryl-ethanol), which is able to interact by solvation and to split the NMR signals of the enantiomers.[25] This was possible with the addition of a quantity of TFAE in a 250 : 1 molar ratio, and the best separation was observed at -53 °C. Figure **16** is an example of a triplet of the phenothiazine. Hence, this experiment proves the possibility to obtain two enantiomeric forms from this compound.
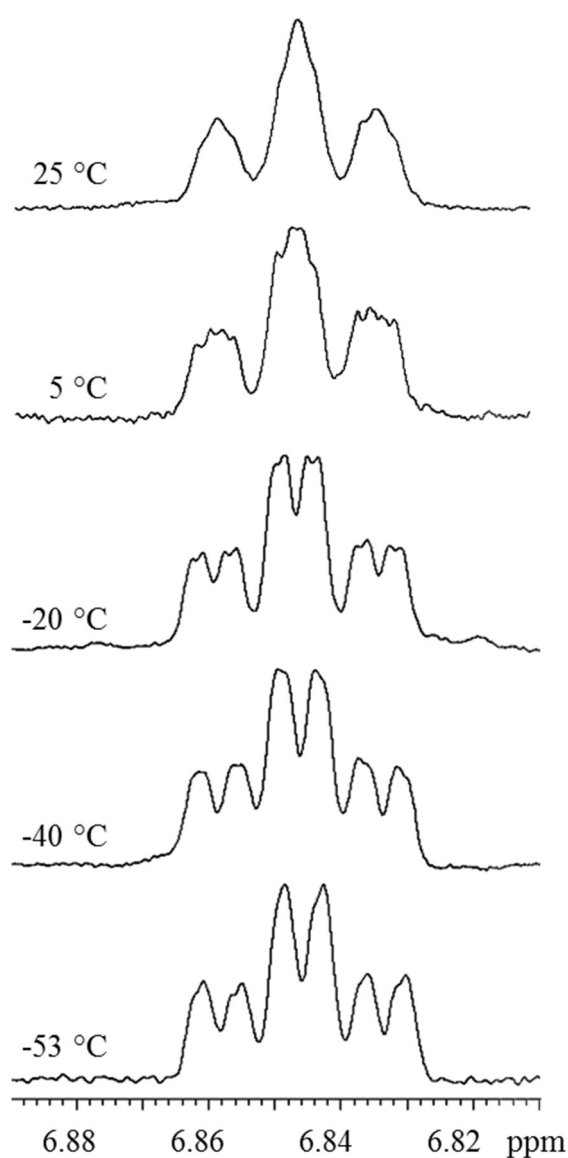
*Figure 16 ^{1}H NMR spectrum of **2c** with Pirkle's alcohol in CD$_2$Cl$_2$ at 600 MHz*

3.2.7 Dynamic NMR and 1D-EXSY of 1b

The NMR spectrum of compounds **1b**, and **1c** present at ambient temperature very broad aryl signals. This could be due to the presence of diastereomeric conformations in a slow exchange. As shown in the previous DFT calculations, **1b** is the only compound where the population of the *syn* conformations is not negligible (estimated energy difference was 0.71 kcal/mol and 1.71 kcal/mol). Hence, we decided to analyse this molecule with both the DNMR and EXSY techniques.

The EXSY analysis was conducted at three temperatures (+80 °C, +85 °C and +90 °C), in order to make the **Phen-flip** fast. In this situation the only visible conformational exchange is the 2-methyl-naphthyl rotation that converts the *anti* conformation to the *syn* and *viceversa*. In figure **17** it is shown the EXSY spectra at +90 °C, with the irradiation of the methyls in *anti* conformations. It has to be noted that saturation transfer occurring in EXSY lead to the grow of a single signal for the two *syn* conformations because at high temperature the **Phen-flip** is fast.
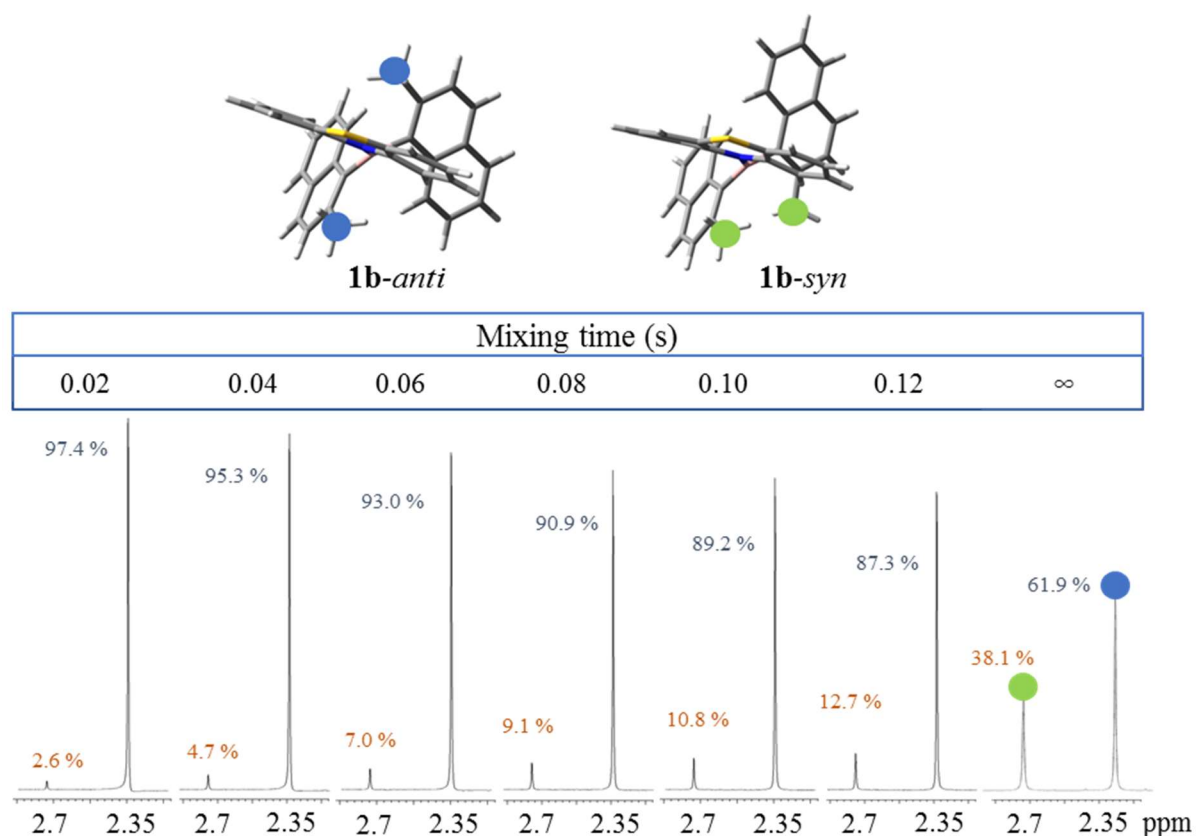
*Figure 17 EXSY of **1b-anti** at +90 °C of the methyl ^1H signal in $C_2D_2Cl_4$ at 600 MHz. The top 3D images have the phenothiazine in a planar conformation to account for the fast **Phen-flip** occurring at high temperatures.*

In this case, since this process brings to the formation of two diastereomers with different energies, the equilibrium value of $C_{irr\ eq}$ depends on the energy difference between them. Hence, there will be two values of k and $\Delta G^{\neq}$, one for the forward reaction from the *anti* to the *syn* (k_{syn}, $\Delta G^{\neq}_{syn}$) and one for the backward (k_{anti}, $\Delta G^{\neq}_{anti}$), being $\Delta G^{\circ} = \Delta G^{\neq}_{anti} - \Delta G^{\neq}_{syn}$. The equation is the following:

$$\ln(C_{irr} - C_{irr\ eq}) = -(k_{anti} + k_{syn}) \cdot t_{mix} + \ln(C_{irr\ 0} - C_{irr\ eq})$$

From the experiments, we obtained the following graphs.
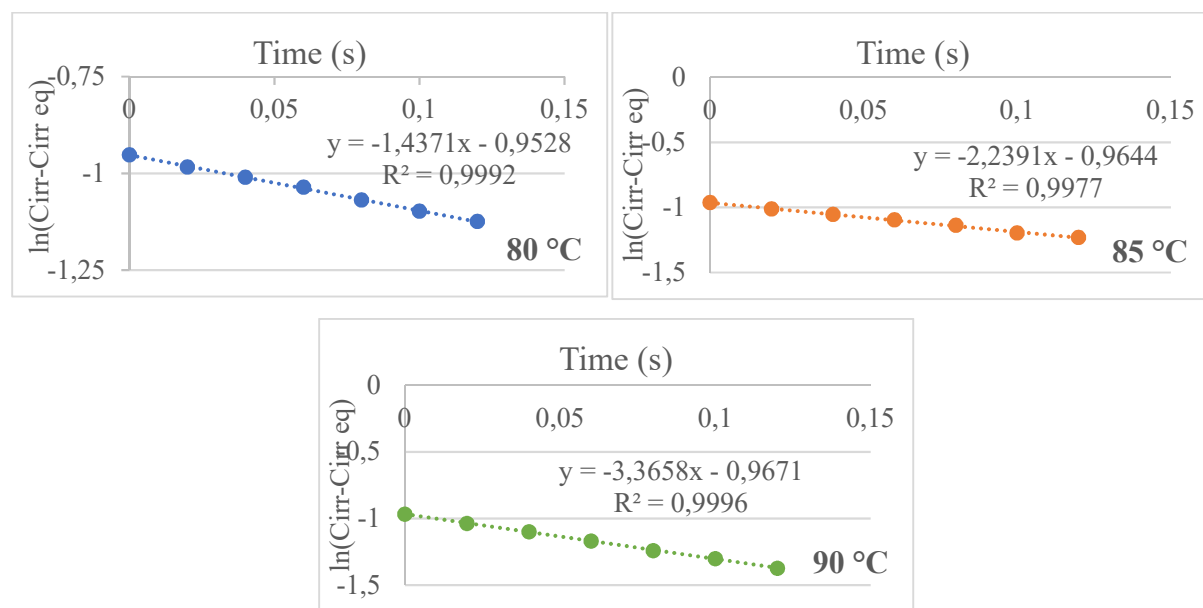
*Graphic 2 Kinetic equations from EXSY analysis for different temperatures for compound **1b***

From this analysis $\Delta G^{\neq}_{anti}$ was 20.8 ± 0.2 kcal/mol and $\Delta G^{\neq}_{syn}$ was 21.2 ± 0.2 kcal/mol, which are consistent with the calculated value of **TS1-1rf** for the rotation of the 2-methyl-naphtyl (21.77 kcal/mol). Moreover, it shows how the formation of the *anti* conformation is more favoured than the *syn* one.

For a further analysis, DNMR study was used to evaluate the **Phen-flip** energy barrier, since when it is completely frozen it will be possible (if they are both populated) to distinguish the two *syn* conformations (**GS2-syn** and **GS3-syn**) and the **GS1-anti**. The ^{1}H spectrum recorded at -56 °C shows four signals for a single hydrogen of the aromatic region (Figure **18**).
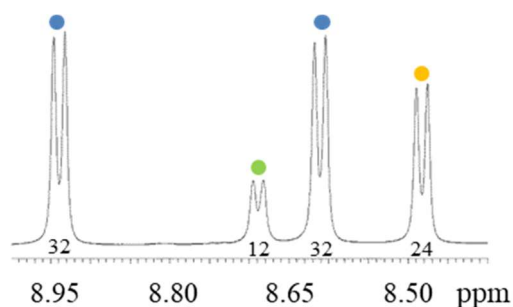
*Figure 18 ¹H NMR spectrum of **1b** of the 1 phenothiazine ¹H signal in C₂D₂Cl₄ at 600 MHz at -56 °C. Blue dots are anti conformation. Orange and green are the two syn conformations.*

The *anti* conformation can be easily assigned because the two 2-methyl-naphthyl are magnetically not equivalent, thus displaying two different signals for the methyls (Figure **19**) and for the aromatic region (Figure **18**) with the same integral (blue dots). On the other hand, both the *syn* conformations belong to the C_s symmetry group and show a signal for the two methyls of each conformation, just like the aromatic region (orange and green dots). The conformational ratio derived from integration was 64:24:12 (**GS1-*anti*:GS2-*syn*:GS3-*syn***). The simulation of the conformational process was more conveniently done on the 2-Methyl signal, as shown in Figure **19**. A $\Delta G^{\neq}$ of 12.4 ± 0.15 kcal/mol was derived for the **Phen-flip** process both in the *anti* and in the *syn* conformations.
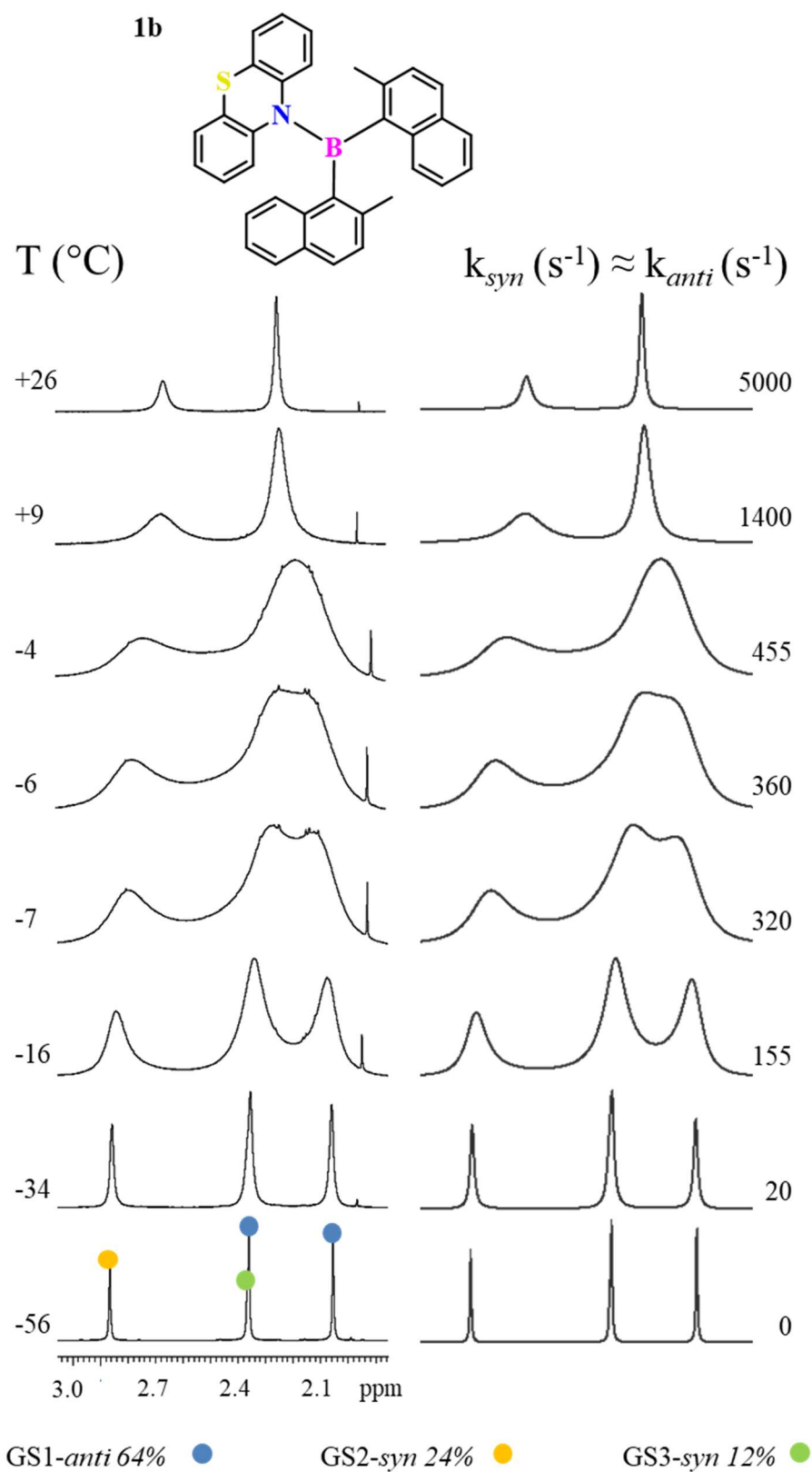
*Figure 19 DNMR of **1b**. Left: temperature dependence of the methyls ^1H signal in $C_2D_2Cl_4$ at 600 MHz. Right: line shape simulation obtained with the rate constants reported.*

3.2.8 EXSY of 2b

The EXSY analysis for compound **2b** was quite challenging, since, unlike the previous two molecules, both phenomena of **Phen-flip** and **B-N** rotation occurs in the same temperature range, and the asymmetry of 2-methylnaphthalene make them both observable. The exchange of protons can happen following four pathways:

- Two Phen-flips
- Two Phenothiazine rotations
- One Phen-flip and one phenothiazine rotation of the same ring
- One Phen-flip on a ring and one phenothiazine rotation of the other ring

Hence, the irradiation of a single internal proton (the closest to the nitrogen) of the phenothiazine raises other three signals.

First of all, it was necessary to assign by NOE the hydrogen chemical shifts of the four hydrogens in position ortho to the two nitrogens. Saturation of the methyl of the 2-methyl-naphthyl-ring yielded NOE on the four hydrogens with different integrals: it was then possible to derive the distance between the four protons and the methyl and, using the model of the ground state, we were able to assign the chemical shifts of each proton.

Green 5.95 ppm
Blue 7.13 ppm
Red 6.26 ppm
Purple 7.25 ppm

$$\frac{d_1}{d_2} = \frac{\sqrt[6]{\eta_2}}{\sqrt[6]{\eta_1}}$$

Anti-en1
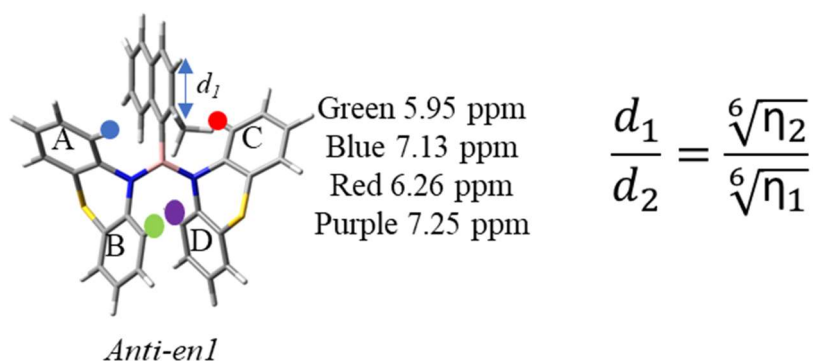
Figure 20 Chemical shift of phenothiazine protons of 2b

The equation in Figure **20** was applied, were d_1 was the distance between the methyl and H-3 the naphthyl ring, η_1 is the integral of this proton when NOE is made on the methyl, η_2 is the integral of the proton on the phenothiazine ring and the unknown d_2 is the distance between the phenothiazine proton and the methyl.

The proton we decided to irradiate for the EXSY experiment was the one at 5.95 ppm at two temperatures (+51 °C and +56 °C) and the other three protons raised in the following ascending order: 6.26 ppm, 7.25 ppm and 7.13 ppm. Thus, the signal at 7.13 ppm is the one

with the faster exchange, corresponding to the lower energy barrier. The exchange of a single signal with the other three implies that both phenothiazine flip and B-N rotation occur with similar rates. Moreover, since there is more than one motion which happens at the same time, to approach the data to a kinetics of the first order only the first mixing times should be taken into account to estimate the $\Delta G^{\neq}$ of the process. The obtained results are reported in Table **7**.

Table 7 Free energy values for any exchanged proton

	7.25 ppm	*7.13 ppm*	*6.26 ppm*
$\Delta G^{\neq}$ (kcal/mol)	19.2	19.0	19.3

To better understand the correspondence between exchanged protons and related motion we represented with a simplified Figure **21** all the possible combinations.

Anti-en1   Phenothiazine Rotation A-B   syn   Phenothiazine Rotation C-D   Anti-en2
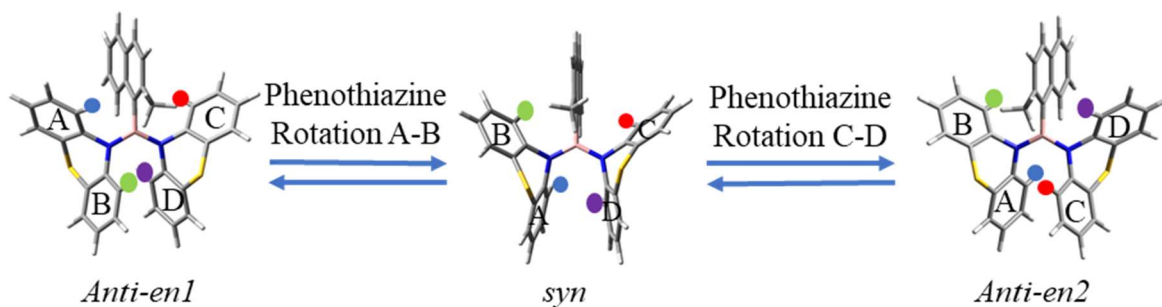
Green 5.95 ppm → Green 6.26 ppm
Blue 7.13 ppm   Blue 7.25 ppm
Red 6.26 ppm ← Red 5.95 ppm
Purple 7.25 ppm   Purple 7.13 ppm

Anti-en1   Phenothiazine Rotation A-B   syn   Phenothiazine Flip A-B   Anti-en1
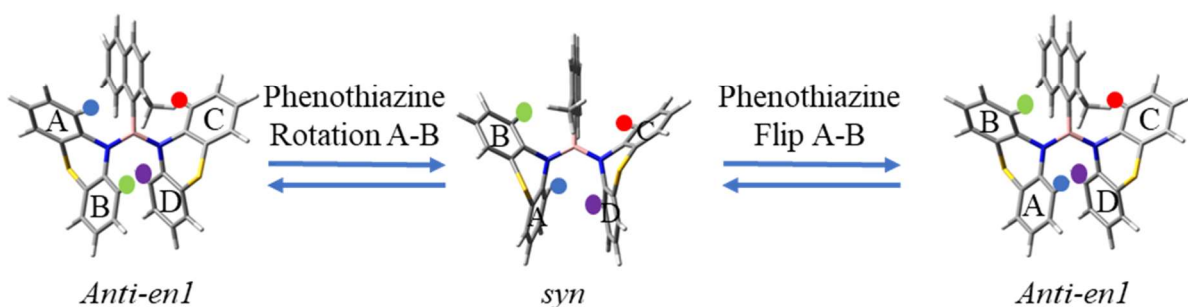
Green 5.95 ppm → Green 7.13 ppm
Blue 7.13 ppm ← Blue 5.95 ppm
Red 6.26 ppm   Red 6.26 ppm
Purple 7.25 ppm   Purple 7.25 ppm

Anti-en1   Phenothiazine Rotation A-B   syn   Phenothiazine Flip C-D   Anti-en2
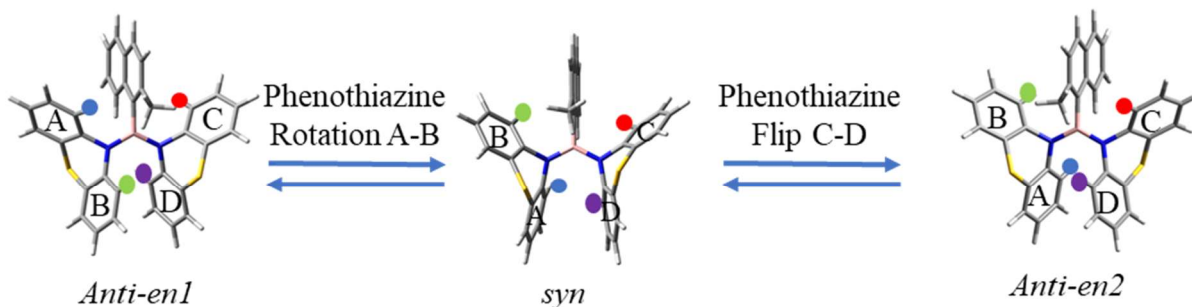
Green 5.95 ppm → Green 6.26 ppm
Blue 7.13 ppm   Blue 7.25 ppm
Red 6.26 ppm   Red 7.13 ppm
Purple 7.25 ppm ← Purple 5.95 ppm

43
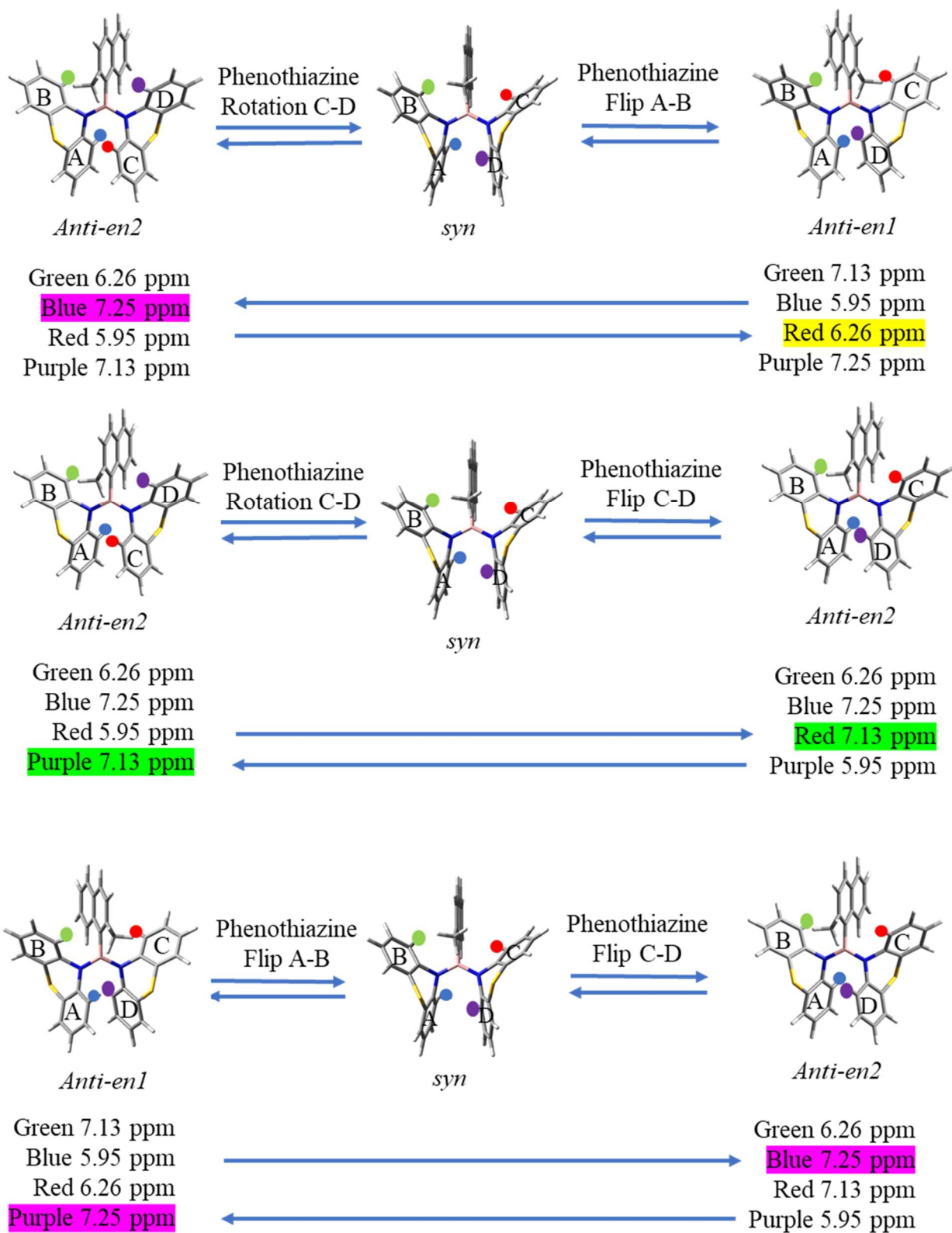
Figure 21 Correspondence between exchanged protons and related motions

To summarise the results which came from this analysis is that the most favourable motion is the one related to the rotation and flip of a single phenothiazine (7.13 ppm) and it doesn't cause the enantiomerization of the compound. The rotation of both phenothiazines causes the enhancing of the signal at 6.26 ppm, while the double **Phen-flip** is related to the signal at 7.25 ppm. At the same time, the combination of one **Phen-flip** and rotation of the other phenothiazine causes the exchange either with 6.26 ppm or with 7.25 ppm. Hence, from this data it is not easy to define the accurate value of energy on a single kind of motion. Nevertheless, we can confirm that phenothiazine rotation and Phen-flip are similar in energy in the order of 19 kcal/mol.

To sum up, none of the synthetized molecule has a sufficient energy barrier to have a single conformer at +25 °C. **2b** and **2c** are both characterized by phenomena of **Phen-flip** and Phenothiazine rotation, since they are energetically similar. In the case of **2b** the only experimentally observable is the rotation, while in the study of **2c** there is a coexistence of both. The 2-methylnaphthyl or anthracenyl rotation are too steric hindered to happen.

For the molecule **1c**, it was possible to study the energy barrier related to the **Phen-flip**, but it cannot be excluded also the presence of phenothiazine and anthracenyl rotation, even if they are not experimentally observable. For compound **1b** it was determined both the energy barrier of the naphthyl rotation (with EXSY), and the **Phen-flip** with DNMR.

All the values obtained are well correlated to those obtained with the DFT calculation.

4 Fluorescence Analysis

For the fluorescence analysis of compound **2b** and **2c**, four solutions were prepared for both compounds with four different solvents (acetonitrile, toluene, hexane and THF). The normalized fluorescence spectra were recorded with a wavelength of excitation of 290 nm for **2b** and 350 nm for **2c**. For **2b**, the solutions were $2.2 \cdot 10^{-5}$ M, while in case of **2c** they were $5.9 \cdot 10^{-5}$ M. This study shows that both molecules show solvatochromic properties. In particular, **2b** shows a red shift with the gradual increase in solvent polarity from hexane to acetonitrile, as shown in Graphic **3**.
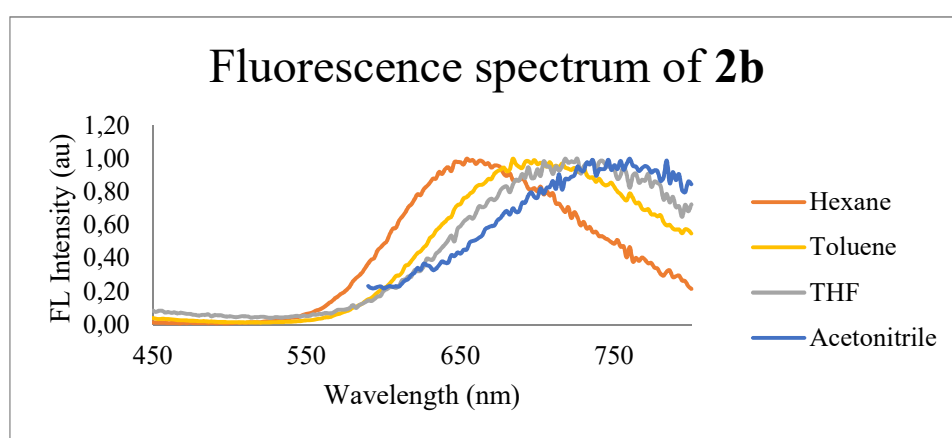
*Graphic 3 Fluorescence spectrum of **2b***

On the contrary, compound **2c** shows a very different situation since it has three maxima of fluorescence and the sequence of the solvents doesn't follow a polarity order. The presence of multiple maxima could be probably related to some impurities or to a different behaviour of various parts of the molecule, such as the anthracenyl group. The trend is reported in Graphic **4**.
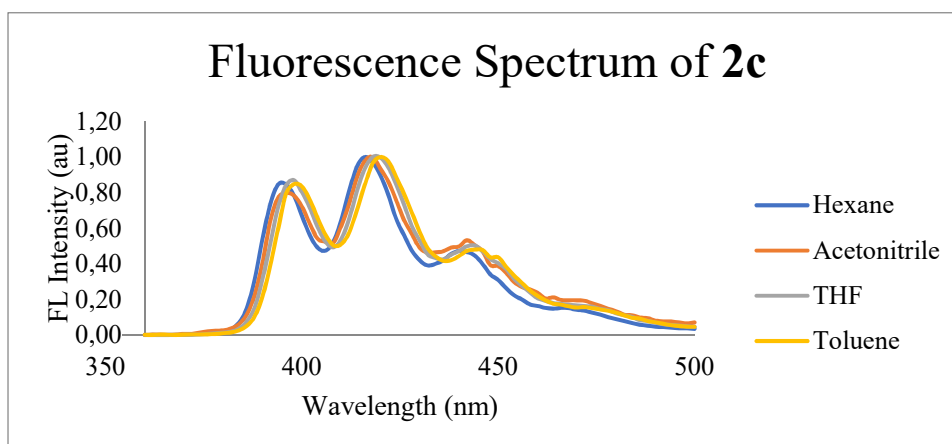
*Graphic 4 Fluorescence spectrum of **2c***

46

5 Conclusions

Our work was focused on a research of good way of synthesis for bis-phenothiazine-aryl-boranes compounds **2b** and **2c**. In the future developments, it would be interesting to improve every reaction step in order to obtain a greater yield and to minimise all the by-products. Products **2b** and **2c**, and also the coproducts **1b** and **1c** were characterized with multiple techniques, such as NMR, mass spectroscopy and X-rays on single crystals.

Successively, we have made a deep study on the conformational behaviour of these molecule, analysing all the possible Ground and Transition States with the use of DFT calculations. Then, with experimental analysis, such as DNMR and EXSY, it was possible to determine the experimental energy barriers of the main transitions (Table **8**).

Table 8 Summary of the final results

$\Delta G^{\ddagger}$ *(kcal/mol)*	1b		1c		2b		2c	
	$\Delta G^{\ddagger}_{cal}$	$\Delta G^{\ddagger}_{exp}$	$\Delta G^{\ddagger}_{cal}$	$\Delta G^{\ddagger}_{exp}$	$\Delta G^{\ddagger}_{cal}$	$\Delta G^{\ddagger}_{exp}$	$\Delta G^{\ddagger}_{cal}$	$\Delta G^{\ddagger}_{exp}$
Phen-Rot	20.6	//	20.0	//	16.6	~ 19.0	16.3	17.7
Phen-Flip	11.8 *syn* 12.3 *anti*	12.4 *syn* 12.4 *anti*	11.8	13.1	18.6	~ 19.0	18.9	//
Aryl-rotation	21.8	20.8	21.6	//	-	//	-	//

// not determinable; - not found; ~ ±0.5 kcal/mol.

After that, we have conducted the fluorescence analysis which showed the solvatochromic properties of compounds **2b** and **2c**.

In the future developments it would be interesting to deepen the use of these compounds as potential smart materials, making some trials to verify their effective role in real applications.

6 Experimental Section

6.1 Materials

The commercially available reagents are the following: 9-bromoanthracene, 1-bromo-2-methylnaphthalene, magnesium, iodine, boron trifluoride diethyl etherate, phenothiazine, potassium bis(trimethylsilyl)amide 0.5 M in toluene, *n*-butyl lithium 1.6 M in hexane, THF, diethyl ether and toluene. The dried solvents are obtained by distillation: toluene is distilled on calcium hydride and stored anhydrous on molecular sieves, while diethyl ether and THF are distilled with sodium/benzophenone. Deuterated solvents for NMR spectra are commercially available. All the reactions are conducted under a constant flux of N_2, dried for transfer through a trap of silica and KOH.

6.2 Instruments

All the glassware is made anhydrous, leaving it for about four hours in a heater at +70 °C. For the chromatography, the following stationary phases are used:

♦ Column chromatography: Silica gel (Merck Grade 9385) 60 Å (230-400 mesh Sigma Aldrich)

♦ TLC plates: Silica gel 60 F_{254}, aluminium sheets

For the further purification of the products it is used a semipreparative HPLC Waters™ 600 with a 254 nm lamp. The columns are the following:

♦ Nova-Pak® (DP – direct phase) Silica 6 μm 19 x 300 mm (20 mL/min) with an eluent mixture of Hexane/DCM = 95 : 5.

♦ Synergi (reverse phase) RP1 250 x 21,20 (20 mL/min) with an eluent mixture of Acetonitrile/H_2O = 97 : 3

Mass spectrum are registered with a spectrometer MICROMASS ZQ 4000 in Electron Spray Ionisation (ESI).

The NMR spectra ^{1}H-NMR, ^{13}C-NMR and ^{11}B-NMR are acquired with Varian Inova 600 (600 MHz).

Fluorescence spectra are made with the spectrometer EDINBURG H620

6.3   Synthesis of 6b and 6c

$$\text{Ar—Br} \quad \xrightarrow[\text{Reflux, 1 h}]{\text{Mg, Et}_2\text{O/Tol 1:1}} \quad \text{ArMgBr}$$

3b, 3c → **6b, 6c**

Ar:

b   **c**
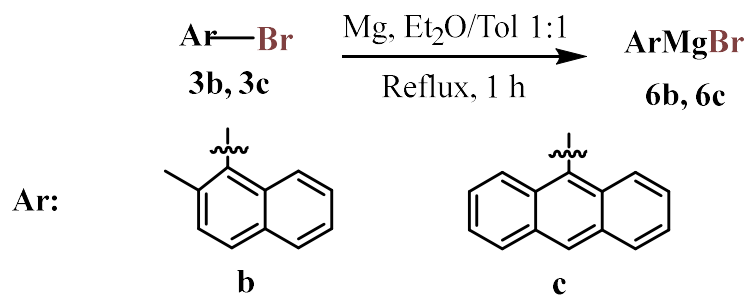
300 mg of magnesium (12.3 mmol) are left stirred into a solution of 10 mL of dry Et₂O and 10 mL of dry toluene for one night in a two-necked flask equipped with a magnetic stir bar. All the solvents are added using a glass syringe through a silicone septum in order to minimize any air infiltration. The day after 1.2 mmol of aryl-bromide are added to the solution (310 mg for 9-Bromoanthracene and 200 µL for 1-bromo-2-methylnaphthalene). A catalytic amount of iodine is added, and we keep on stirring. With a hotplate, the solution is brought to reflux until there is visible a colour change from deep brown to yellow. At this point, we wait for an hour to complete the Grignard reaction and then we let it cool down at room temperature.

6.4   Synthesis of 4b, 4c, 5b and 6b

$$\text{ArMgBr} \quad \xrightarrow[\substack{\text{2) Reflux, 1 h} \\ \text{3) Dried under vacuum}}]{\text{1) BF}_3\text{OEt}_2\text{; toluene; 0 °C}} \quad \text{ArBF}_2 \; + \; \text{Ar}_2\text{BF}$$

6b, 6c   **4b, 4c**   **5b, 5c**
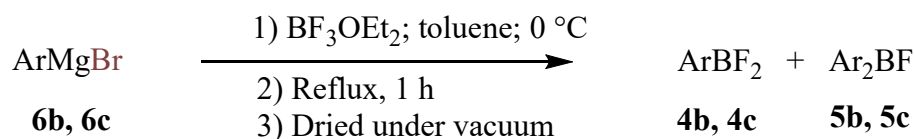
At this point nitrogen flux is switched with a vacuum line, so that all the diethyl ether is removed, and we replace it with other 10 mL of dry toluene. With an ice bath, the solution is cool down to 0 °C and 1.5 mmol of BF₃OEt₂ (185 µL) is added dropwise to the solution. Then, with a hot oil bath we bring it back to reflux for 1 hour and after that, it is cool down at room temperature. The solution is now collected with a syringe and inserted into another two-necked flask with a magnetic stir bar to separate it from the non-reacted magnesium. At this point, all the solution is dried under high vacuum to remove any residual BF₃.

49

6.5 Synthesis of 1b, 1c, 2b and 2c

$$\text{ArBF}_2 \quad + \quad \text{Ar}_2\text{BF} \quad \xrightarrow[\text{2) reflux, overnight}]{\text{KHMDS 0 °C; toluene}}$$

4b, 4c   **5b, 5c**
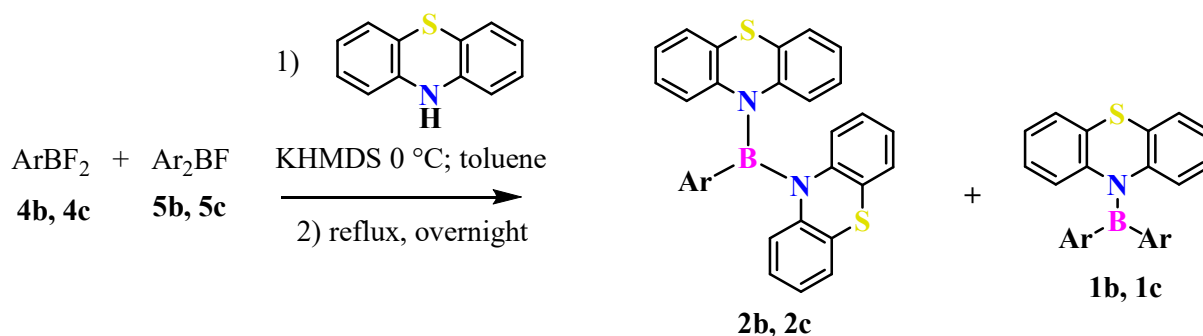
As last step of reaction, 2.5 mmol of phenothiazine (500 mg) are added to the solid mixture of ArBF$_2$ and Ar$_2$BF. Firstly, all the reactants are dissolved adding 10 mL of dry toluene with the magnetic bar stirring. Temperature is increased, in order to favour the dissolving and after that, with a bath of ice it is brought back to 0 °C. At this point, using a syringe 5 ml of KHMDS 0.5 M are added dropwise to the solution. It is observed a sharp yellow colour, due to the formation of the phenothiazine anion. The temperature is increased until reflux and let it react overnight.

6.6 Work-Up

When the reaction is complete the flask is opened at the air and the solution is quenched with CH$_2$Cl$_2$. After that, the solution is filtered under vacuum with a porous separator and a plug of Celite® to be sure to remove any inorganic salt. In the end, the solution is dried under vacuum and prepared for the purification with a chromatographic column. The silica gel column chromatography is eluted with a solution of *n*-Hexane/CH$_2$Cl$_2$ with an 8:2 ratio. For a further purification, the compounds are eluted with a semipreparative HPLC, with the possibility to use either a reverse phase or a direct phase column, as reported above.

6.7 Characterization of compounds 2b, 2c, 1b and 1c

Bis-phenothiazine-2-methylnaphthyl-borane (2b)

^{1}H-NMR (600 MHz, $C_2D_2Cl_4$ 6.00 ppm, +25 °C): δ 2,3 (s, $3H_{Me}$), 5.98 (d, J = 8,4 Hz, 1H), 6.29 (d, J = 7,89 Hz, 1H), 6.35 (t, J = 7,51 Hz, 1H), 6.44 (t, J = 7,10 Hz, 1H) 6.62 (t, J = 7,10 Hz, 1H), 6.66-6.75 (m, $2H_{Ar}$), 6.82 (t, J = 7.78 Hz, 2H), 6.87 (t, J = 7.42 Hz, 1H), 7.10 (d, J = 8.13 Hz, 1H), 7.13-7.19 (m, $4H_{Ar}$), 7.24-7.29 (m, $2H_{Ar}$), 7.30-7.35 (m, $2H_{Ar}$), 7.65 (d, J = 8.14 Hz, 1H), 7.68 (d, J = 8.14 Hz, 1H), 7.97 (d, J = 8,14 Hz, 1H).

^{13}C-NMR (150.8 MHz, $C_2D_2Cl_4$, 74.0 ppm, +25 °C): δ 22.0 (CH_3), 74.3 (CH), 124.1 (CH), 124.3 (CH), 124.4 (CH), 125.0 (CH), 125.0 (CH) 125.2 (CH), 125.3 (CH), 125.6 (CH), 125.7 (CH), 125.8 (CH), 126.0 (CH), 126.4 (CH), 127.0 (CH), 127.1 (CH), 127.2 (CH), 127.4 (CH), 127.5 (CH) 127.9 (CH), 127.9 (CH), 128.0 (CH), 131.0 (Cq), 133.3 (Cq), 133.5 (Cq), 133.7 (Cq), 133.7$_5$ (Cq), 135.4 (Cq), 137.9 (Cq), 144.4 (Cq), 144.5 (Cq), 144.5$_3$ (Cq), 144.6 (Cq).

^{11}B-NMR (192.4 MHz, $C_2D_2Cl_4$, $BF_3\cdot Et_2O$, 0 ppm, +25 °C): δ 31.8

Bis-phenothiazine-anthracenyl-borane (2c)

^{1}H-NMR (600 MHz, CD_2Cl_2, 5.32 pm, +25 °C): δ 5.85 (dd, J = 8.11; 1.15 Hz; 2H), 6.04 (ddd, J = 8.34; 7.29; 1.41 Hz; 2H), 6.55 (td, J = 7.42; 1.28 Hz; 2H), 6.68 (td, J = 7.63; 1.45 Hz; 2H), 6.84 (td, J = 7.48; 1.31 Hz; 2H); 7.15 (dd, J = 7.44; 1.30 Hz; 2H), 7.22 (dd, J = 7.61; 1.30 Hz; 2H), 7.24 (dd, J = 7.82; 1.09 Hz; 2H), 7.31-7.37 (m, $4H_{Ar}$), 7.86-7.92 (m, $2H_{Ar}$), 8.27-8.31 (m, $2H_{Ar}$), 8.33 (s, 1H).

^{13}C-NMR (150.8 MHz, CD_2Cl_2, 54.0 ppm, +25 °C): δ 123.9 (CH), 124.6 (CH), 124.8 (CH), 125.1 (CH), 125.2 (CH), 125.2$_4$ (CH), 125.7 (CH), 126.7 (CH), 126.9 (CH), 127.1 (CH), 127.3 (CH), 128.4 (CH), 128.5 (CH), 130.8 (Cq), 133.6 (Cq), 133.9 (Cq), 134.0 (Cq), 144.7 (Cq), 144.9 (Cq).

^{11}B-NMR (192.4 MHz, CD_2Cl_2, $BF_3\cdot Et_2O$, 0 ppm, +25 °C): δ 32.2

Bis-2-methyl-naphtyl-phenothiazine-borane (1b)

^{1}H-NMR (400 MHz, Acetonitrile, 1.96 ppm, +25 °C): δ 2.31 (s, 3H), 2.65 (bs, 3H), 6.67 (t, J = 7.54 Hz 1H) 6.73 (t, J = 7.76 Hz, 1H) 6.88 (t, J = 7.32 Hz, 1H), 6.94 (t, J = 7.54 Hz, 1H),

7.09 (d, J = 8.24, 1H), 7.16 (bs, 1H), 7.20 (broad, 2H), 7.28 (d, J = 7.91, 1H), 7.32 (bs, 3H) 7.37 (bs, 1H), 7.50 (bs, 1H) 7.62 (d, J = 7.81, 2H) 7.71 (bs, 2H), 8.62 (bs, 1H), 8.75 (bs, 1H).

Bis-anthracenyl-phenothiazine-borane (1c)

^{1}H-NMR (600 MHz, CD$_2$Cl$_2$, 5.32 pm, +25 °C): δ 6.55 (t, J = 7.83, 2H), 6.86 (t, J = 7.83, 2H), 7.27 (d, J = 7.66, 2H), 7.35 (bs, 8H), 7.44 (d, J = 8.24, 2H), 7.90 (bs, 4H), 8.31 (s, 2H), 8.94 (bs, 4H).

7 Bibliography

(1)   Mellerup, S. K.; Wang, S. Boron-Based Stimuli Responsive Materials. *Chem. Soc. Rev.* **2019**, *48* (13), 3537–3549. https://doi.org/10.1039/c9cs00153k.

(2)   Beharry, A. A.; Woolley, G. A. Azobenzene Photoswitches for Biomolecules. *Chem. Soc. Rev.* **2011**, *40* (8), 4422–4437. https://doi.org/10.1039/c1cs15023e.

(3)   Cui, J.; Kwon, J. E.; Kim, H. J.; Whang, D. R.; Park, S. Y. Smart Fluorescent Nanoparticles in Water Showing Temperature-Dependent Ratiometric Fluorescence Color Change. *ACS Appl. Mater. Interfaces* **2017**, *9* (3), 2883–2890. https://doi.org/10.1021/acsami.6b13818.

(4)   Liu, L.; Wang, X.; Wang, N.; Peng, T.; Wang, S. Bright, Multi-Responsive, Sky-Blue Platinum(II) Phosphors Based on a Tetradentate Chelating Framework. *Angew. Chemie - Int. Ed.* **2017**, *56* (31), 9160–9164. https://doi.org/10.1002/anie.201705785.

(5)   Alemani, M.; Peters, M. V.; Hecht, S.; Rieder, K. H.; Moresco, F.; Grill, L. Electric Field-Induced Isomerization of Azobenzene by STM. *J. Am. Chem. Soc.* **2006**, *128* (45), 14446–14447. https://doi.org/10.1021/ja065449s.

(6)   Yu, X.; Wang, Z.; Jiang, Y.; Shi, F.; Zhang, X. Reversible PH-Responsive Surface: From Superhydrophobicity to Superhydrophilicity. *Adv. Mater.* **2005**, *17* (10), 1289–1293. https://doi.org/10.1002/adma.200401646.

(7)   Kocak, G.; Tuncer, C.; Bütün, V. PH-Responsive Polymers. *Polym. Chem.* **2017**, *8* (1), 144–176. https://doi.org/10.1039/c6py01872f.

(8)   Vyšniauskas, A.; Qurashi, M.; Gallop, N.; Balaz, M.; Anderson, H. L.; Kuimova, M. K. Unravelling the Effect of Temperature on Viscosity-Sensitive Fluorescent Molecular Rotors. *Chem. Sci.* **2015**, *6* (10), 5773–5778. https://doi.org/10.1039/c5sc02248g.

(9)   Martínez-Máñez, R.; Sancenón, F. *Fluorogenic and Chromogenic Chemosensors and Reagents for Anions*; 2003; Vol. 103. https://doi.org/10.1021/cr010421e.

(10)   Zhao, Q.; Li, F.; Huang, C. Phosphorescent Chemosensors Based on Heavy-Metal Complexes. *Chem. Soc. Rev.* **2010**, *39* (8), 3007–3030. https://doi.org/10.1039/b915340c.

(11)   Bandara, H. M. D.; Burdette, S. C. Photoisomerization in Different Classes of Azobenzene. *Chem. Soc. Rev.* **2012**, *41* (5), 1809–1825. https://doi.org/10.1039/c1cs15179g.

(12)   Sagara, Y.; Kato, T. Mechanically Induced Luminescence Changes in Molecular Assemblies. *Nat. Chem.* **2009**, *1*, 605.

(13)   Arivazhagan, C.; Maity, A.; Bakthavachalam, K.; Jana, A.; Panigrahi, S. K.; Suresh, E.; Das, A.; Ghosh, S. Phenothiazinyl Boranes: A New Class of AIE Luminogens with Mega Stokes Shift,

Mechanochromism, and Mechanoluminescence. *Chem. - A Eur. J.* **2017**, *23* (29), 7046–7051. https://doi.org/10.1002/chem.201700187.

(14) Dong, H.; Li, W.; Sun, J.; Li, S.; Klein, M. L. Understanding the Boron-Nitrogen Interaction and Its Possible Implications in Drug Design. *J. Phys. Chem. B* **2015**, *119* (45), 14393–14401. https://doi.org/10.1021/acs.jpcb.5b07783.

(15) Pasteur, L. Dissymétrie Moléculaire. *Ann. Chim. Phys.* **1848**, *24*, 442–459.

(16) Reist, M.; Carrupt, P. A.; Francotte, E.; Testa, B. Chiral Inversion and Hydrolysis of Thalidomide: Mechanisms and Catalysis by Bases and Serum Albumin, and Chiral Stability of Teratogenic Metabolites. *Chem. Res. Toxicol.* **1998**, *11* (12), 1521–1528. https://doi.org/10.1021/tx9801817.

(17) Oki, M. *Top. Stereochem.*; **1983**, *14*, 1-81.

(18) Laplante, S.P.; Edwards, P. J.; Fader, L.D.; Jakalian, A.; Hucke, O. Revealing Atropisomer Axial Chirality in Drug Discovery. *ChemMedChem* **2011**, *6*, 503–513.

(19) Mislow, K. Stereochemical Consequences of Correlated Rotation in Molecular Propellers. *Acc. Chem. Res.* **1976**, *9* (1), 26–33. https://doi.org/10.1021/ar50097a005.

(20) Zhang, Y.; Calupitan, J. P.; Rojas, T.; Tumbleson, R.; Erbland, G.; Kammerer, C.; Ajayi, T. M.; Wang, S.; Curtiss, L. A.; Ngo, A. T.; et al. A Chiral Molecular Propeller Designed for Unidirectional Rotations on a Surface. *Nat. Commun.* **2019**, *10* (1), 3742. https://doi.org/10.1038/s41467-019-11737-1.

(21) Neena, K. K.; Sudhakar, P.; Dipak, K.; Thilagar, P. Diarylboryl-Phenothiazine Based Multifunctional Molecular Siblings. *Chem. Commun.* **2017**, *53* (26), 3641–3644. https://doi.org/10.1039/c6cc09717k.

(22) Gao, Wei; Wang, Xiangcheng; Zhang, Lei; Niu, Jinghua; Lu, Yan; Fan, Changxuan; Huang, Gaojun; An, P. Aromatic Heterocyclic Compound and Organic Light-Emitting Display Device. CN108727405, **2018**.

(23) Antony, J.; Grimme, S. Density Functional Theory Including Dispersion Corrections for Intermolecular Interactions in a Large Benchmark Set of Biologically Relevant Molecules. *Phys. Chem. Chem. Phys.* **2006**, *8* (45), 5287–5293. https://doi.org/10.1039/b612585a.

(24) Casarini, D.; Lunazzi, L.; Mazzanti, A. Recent Advances in Stereodynamics and Conformational Analysis by Dynamic NMR and Theoretical Calculations. *European J. Org. Chem.* **2010**, *2* (11), 2035–2056. https://doi.org/10.1002/ejoc.200901340.

(25) Pirkle, W. H.; Sikkenga, D. L.; Pavlin, M. S. Nuclear Magnetic Resonance Determination of Enantiomeric Composition and Absolute Configuration of γ-Lactones Using Chiral 2,2,2-Trifluoro-1-(9-Anthryl)Ethanol. *J. Org. Chem.* **1977**, *42* (2), 384–387. https://doi.org/10.1021/jo00422a061.